GEOTHERMAL ENERGY IN COLOMBIA: GEOLOGICAL FRAMEWORK, EXPLORATION ADVANCES, AND PROSPECTS FOR DEVELOPMENT

ABSTRACT

Through a systematic review of published studies and technical reports, this work analyzes the current state of geothermal energy in Colombia, its limitations, environmental implications, regulatory progress, and development perspectives. Exploration has focused mainly on high-enthalpy volcanic systems such as Nevado del Ruiz, Azufral, Paipa, and Tufiño–Chiles–Cerro Negro, where geological, geochemical, geophysical, and hydrothermal evidence confirms reservoir temperatures above 200 °C and preliminary potentials ranging between 20 and 200 MWe per site. In parallel, conduction-dominated systems in sedimentary basins, particularly in the Llanos, have gained attention through oilfield co-production pilots. These initiatives demonstrate the feasibility of binary ORC plants (200–320 kWe) and estimate an additional technical potential of 170–287 MWe.

At the national scale, the Colombian Geological Survey estimates a preliminary potential of ~1170 MWe from convection-dominated systems, with projections of up to ~800 MWe installed by 2050 under the National Energy Plan. Recent milestones include the first geothermal electricity generation in Campo Maracas (Casanare, 2024) and the concession for advanced exploration in the Azufral volcano (2025). Regulatory advances—Law 2099 (2021), Decree 1318 (2022), and Decree 1598 (2024)—have consolidated geothermal energy as an independent source within Colombia's energy portfolio, creating clearer conditions for investment.

Despite promising prospects, technological, financial, and exploratory uncertainties remain high, highlighting the need for drilling, reservoir characterization, and innovative approaches such as machine learning to reduce exploration risk. Overall, geothermal energy represents a strategic opportunity to diversify Colombia's energy matrix, contributing stable, low-emission baseload power and supporting the country's long-term sustainability and energy transition goals. It is important to note that these estimates are approximate and based on data collected by the Colombian Geological Survey and studies conducted by various authors over time. Thus, they have a 90% confidence interval with a considerable range and a margin of error that must be reduced. For the next few years, a considerable increase in geothermal installed capacity in the world, and consequently, in the generation and supply of electricity is predicted. Colombia estimates a preliminary capacity of 1170 MWe, framed within the national energy ideology and subject to more detailed and rigorous studies for the future to consolidate geothermal projects and reduce technological and financial uncertainty.

1 Introduction

Geothermal energy, derived from the Greek words geos (earth) and thermos (heat), refers both to the science that studies the Earth's internal heat and to the industrial processes that harness it for electricity generation and direct uses such as heating. Globally, geothermal power is a consolidated renewable source: by 2021 the United States led production with 3700 MWe of installed capacity, while Mexico reached 1005 MWe, ranking among the ten countries that surpass 500 MWe (Lund and Toth, 2021). By 2025, global installed capacity is estimated at nearly 17 GW, reflecting sustained growth (IEA, 2024).

Colombia, located on the Pacific Ring of Fire, holds a privileged geodynamic position with significant geothermal potential. Exploration efforts began in 1968 with Italian evaluations of the Nevado del Ruiz volcanic complex (Bona and Coviello, 2016) and were later resumed in 1983 through CHEC pre-feasibility studies. Since 1997, the Colombian Geological Survey (formerly INGEOMINAS) has advanced

geothermal research, complemented by initiatives from utilities such as ISAGEN in the Nevado del Ruiz and Tufiño-Chiles-Cerro Negro areas (Mejía et al., 2014; Salazar et al., 2017). More recently, ECOPETROL (*Empresa Colombiana de Petróleo S.A.*) has tested low-enthalpy applications, while the pilot project at Campo Maracas (Casanare) began operations in 2024, marking the first geothermal electricity produced in the country. Additionally, the Ministry of Mines granted in 2025 a permit for advanced exploration in the Azufral volcanic area, signaling a potential breakthrough for high-enthalpy development (SGC, 2025; ECOPETROL, 2025).

Colombia's electricity matrix continues to be dominated by hydropower and fossil fuels (EIA, 2018), while non-conventional renewable energies such as solar and wind have expanded significantly in recent years. Geothermal energy, although recognized for its potential, is still at an early stage of industrial development. Earlier estimates suggested a technical potential of ~17,400 GWh/year, equivalent to ~20% of the projected national electricity demand by 2025 (Gawell et al., 1999; Salazar et al., 2017). Nevertheless, its current contribution remains minimal, reflecting the early stage of project implementation.

From a regulatory standpoint, Colombia has recently developed a specific framework for geothermal energy. Law 2099 of 2021 formally recognized geothermal as an independent source within the national energy portfolio. This was followed by Decree 1318 of 2022 and Decree 1598 of 2024, which established the technical and environmental guidelines for exploration and exploitation activities. In addition, geothermal development has been included in the 2018–2022 and 2022–2026 National Development Plans, with the Colombian Geological Survey (SGC) designated as the entity responsible for providing the scientific and technical framework to support these initiatives (Alfaro and Rodríguez, 2020). These advances represent important steps toward creating conditions that favor investment and project development.

From a scientific perspective, geothermal potential can be assessed via geothermal gradients and reservoir conditions. The most comprehensive geothermal gradient map (Alfaro et al., 2009) covers ~50% of the national territory, revealing anomalies exceeding 40 °C/km in the Llanos, Catatumbo, and Caguán–Putumayo basins, with local maxima up to 140 °C/km in the Nevado del Ruiz (SGC–ANH, 2009). Subsequent studies refined these patterns: Bachu et al. (1995) for the Llanos Basin, Quintero et al. (2019) in northwestern Colombia, and Matiz-León (2023) using spatial statistics. More recently, Mejía-Fragoso et al. (2024) applied machine learning to predict gradients nationwide, offering a data-driven baseline for exploration in under-sampled regions.

Geothermal energy is considered environmentally advantageous compared to fossil fuels, with lower greenhouse gas emissions, reduced particulate release, and limited land use requirements. Unlike solar or wind, its availability is not subject to climatic fluctuations, and its use is inherently local, strengthening energy sovereignty. These attributes position geothermal energy as a clean and stable complement to Colombia's renewable energy transition.

This manuscript provides an updated and comprehensive review of geothermal exploration in Colombia, emphasizing technical potential, regulatory progress, and the main case studies. The analysis focuses on four key convection-dominated geothermal areas of high relevance: the Azufral Volcano, the Nevado del Ruiz volcanic complex, the Paipa geothermal area, and the Chiles—Cerro Negro volcanic complex (Figure 1). In addition, the review addresses conduction-dominated geothermal systems currently recognized in Colombia.

Sondo Marter
Barronquillor
Cortogeno
Valledujo
Contageno
Valledujo

Figure 1. Figure 3: (a) Diagram of the locations of the regions studied, (b) Photos of the areas studied. Taken and modified from Google Images.

2 Geothermal Energy in Colombia

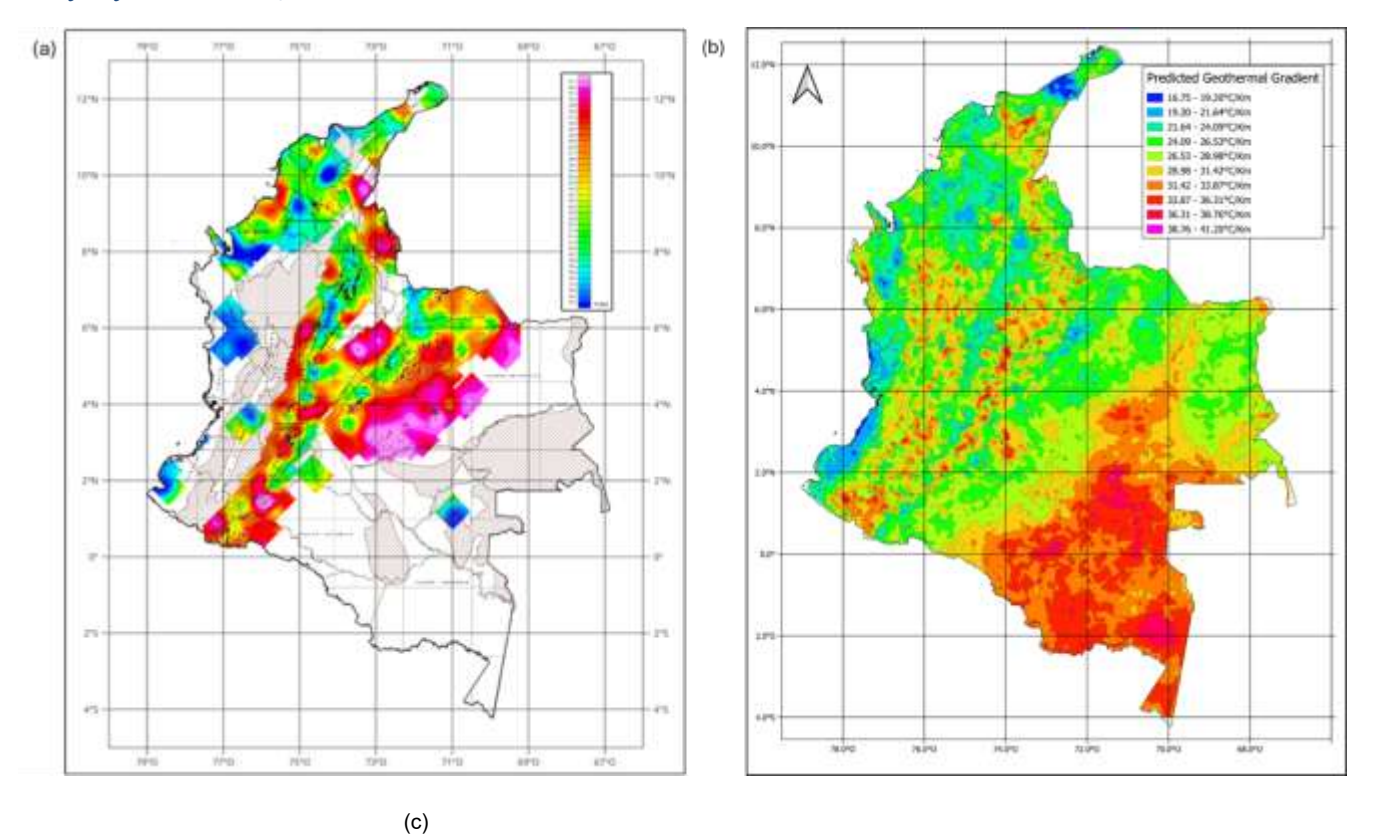
Interest in renewable and sustainable energy has steadily increased worldwide due to concerns about dependence on fossil fuels and their environmental impacts. In Colombia, regulatory policies have promoted investment in non-conventional renewable energies (FNCER) through economic and tax incentives, aiming to diversify the national energy matrix (Alfaro and Rodríguez, 2021). Within this framework, geothermal energy is recognized as a promising, though still emerging, component.

Exploration of geothermal resources in Colombia began in 1968, when the Italian Ente de Electricidad evaluated the Nevado del Ruiz volcanic complex for power generation, commissioned by the Caldas Hydroelectric Power Plant (CHEC) (Bona and Coviello, 2016). These studies were later resumed in 1983 through a pre-feasibility analysis by CHEC, and since 1997 the Colombian Geological Survey (then INGEOMINAS) has conducted systematic geothermal investigations. Utilities such as ISAGEN have complemented these efforts, particularly in the Tufiño–Chiles–Cerro Negro, Nevado del Ruiz, Azufral, and Santa Isabel volcanic systems, as well as in the San Diego Maar and the Maracas Field (Mejía et al., 2014; Salazar et al., 2017).

The first national reconnaissance study was carried out by OLADE in 1982, identifying a pronounced regional thermal anomaly along the Central Cordillera. Later, INGEOMINAS and the National Hydrocarbon Agency (ANH) published in 2009 a geothermal gradient map covering ~50% of the country (Alfaro et al., 2009). This study reported four major anomalies (>40 °C/km) located in the Llanos Orientales, Cordillera Oriental, Caguán–Putumayo, and Catatumbo basins, with maximum gradients of 60–65 °C/km. The highest recorded gradient in Colombia (140 °C/km) corresponds to a geothermal well drilled at Nevado del Ruiz; however, recent estimates from 2023 on refer a 180°C/km gradient for Paipa (Figure 2a and 2b) (Alfaro et al., 2020).

Subsequent studies expanded this knowledge. Alfaro et al. (2020) described convective geothermal systems linked to volcanic and fault-related hydrothermal manifestations as potential geothermal energy and heat sources, estimating an electrical potential of 1170 MWe from these (Figure 2c). More recent works have highlighted methodological advances: statistical approaches to gradient prediction (Matiz-León, 2023), aeromagnetic-based estimates (Quintero et al., 2019), and machine learning methods to forecast gradients nationwide (Mejía-Fragoso et al., 2024) (Figure 2b).

Figure 2. (a) Geothermal gradients map of Colombia. Taken and modified from Alfaro et al., 2009. (b) Predicted geothermal gradient for Colombia, taken from Mejía-Fragoso et al., 2024. (c) Location of the main thermal manifestations of Colombia, modified from SGC (2015)



Volcances ▲

Thermal aprings

0° - 20°

20° - 40°

20° - 40°

20° - 40°

20° - 40°

20° - 40°

20° - 40°

20° - 40°

20° - 40°

20° - 40°

20° - 40°

20° - 40°

20° - 40°

20° - 40°

20° - 40°

20° - 40°

20° - 40°

20° - 40°

20° - 40°

20° - 40°

20° - 40°

20° - 40°

20° - 40°

20° - 40°

20° - 40°

20° - 40°

20° - 40°

20° - 40°

20° - 40°

20° - 40°

20° - 40°

20° - 40°

20° - 40°

20° - 40°

20° - 40°

20° - 40°

20° - 40°

20° - 40°

20° - 40°

20° - 40°

20° - 40°

20° - 40°

20° - 40°

20° - 40°

20° - 40°

20° - 40°

20° - 40°

20° - 40°

20° - 40°

20° - 40°

20° - 40°

20° - 40°

20° - 40°

20° - 40°

20° - 40°

20° - 40°

20° - 40°

20° - 40°

20° - 40°

20° - 40°

20° - 40°

20° - 40°

20° - 40°

20° - 40°

20° - 40°

20° - 40°

20° - 40°

20° - 40°

20° - 40°

20° - 40°

20° - 40°

20° - 40°

20° - 40°

20° - 40°

20° - 40°

20° - 40°

20° - 40°

20° - 40°

20° - 40°

20° - 40°

20° - 40°

20° - 40°

20° - 40°

20° - 40°

20° - 40°

20° - 40°

20° - 40°

20° - 40°

20° - 40°

20° - 40°

20° - 40°

20° - 40°

20° - 40°

20° - 40°

20° - 40°

20° - 40°

20° - 40°

20° - 40°

20° - 40°

20° - 40°

20° - 40°

20° - 40°

20° - 40°

20° - 40°

20° - 40°

20° - 40°

20° - 40°

20° - 40°

20° - 40°

20° - 40°

20° - 40°

20° - 40°

20° - 40°

20° - 40°

20° - 40°

20° - 40°

20° - 40°

20° - 40°

20° - 40°

20° - 40°

20° - 40°

20° - 40°

20° - 40°

20° - 40°

20° - 40°

20° - 40°

20° - 40°

20° - 40°

20° - 40°

20° - 40°

20° - 40°

20° - 40°

20° - 40°

20° - 40°

20° - 40°

20° - 40°

20° - 40°

20° - 40°

20° - 40°

20° - 40°

20° - 40°

20° - 40°

20° - 40°

20° - 40°

20° - 40°

20° - 40°

20° - 40°

20° - 40°

20° - 40°

20° - 40°

20° - 40°

20° - 40°

20° - 40°

20° - 40°

20° - 40°

20° - 40°

20° - 40°

20° - 40°

20° - 40°

20° - 40°

20° - 40°

20° - 40°

20° - 40°

20° - 40°

20° - 40°

20° - 40°

20° - 40°

20° - 40°

20° - 40°

20° - 40°

20° - 40°

20° - 40°

20° - 40°

20° - 40°

20° - 40°

20° - 40°

20° - 40°

20° - 40°

20° - 40°

20° - 40°

20° - 40°

20° - 40°

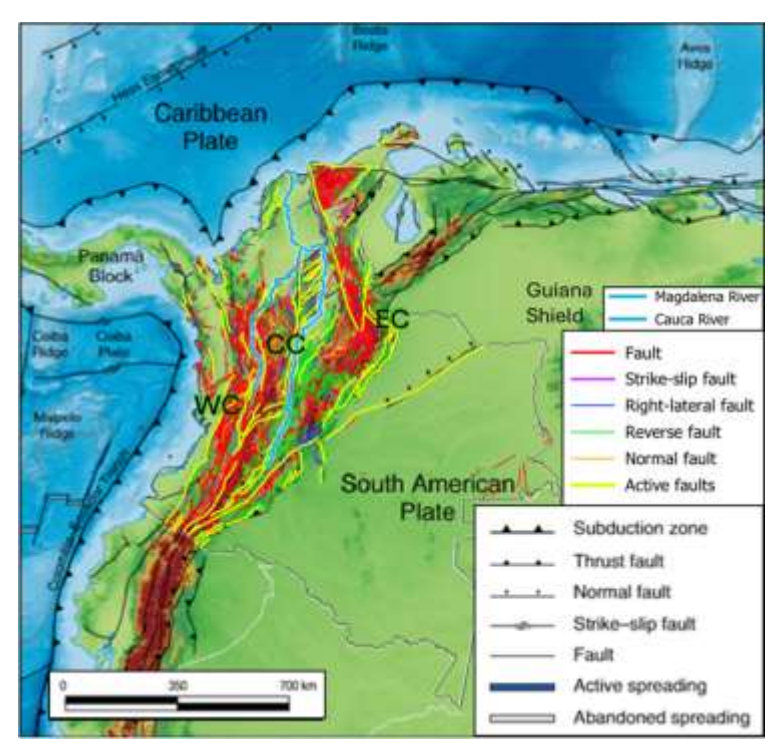
20° - 40°

20°

3 Geological Setting of Colombia

Colombia, located in northwestern South America at the interaction of the Nazca, South American, and Caribbean plates, has a dynamic geological history that extends back to the Precambrian. The Guiana Shield forms part of the ancient continental core, with igneous, volcanic, and metamorphic rocks as old as 1780 Ma (Lobo, 1987). The Andean orogeny, initiated in the Jurassic, continues today, driving tectonic uplift, faulting, and active volcanism. The collision of the Panama Block in the Pliocene closed the Central American Seaway, reshaping ocean circulation and climate (De Porta, 2003) (Figure 3).

Figure 3. Tectonic scheme of Colombia, showing the cordilleras, the different type of faults and the two main rivers. Modified from Gómez-Tapias et al. (2020).



The Colombian Andes are divided into three cordilleras (Lobo, 1987; Gómez-Tapias et al., 2020). The Central Cordillera (CC) consists of polymetamorphic basements intruded by plutons from the Permian to Cenozoic, overlain by Cretaceous volcaniclastic and marine rocks, and crowned by Neogene–Quaternary volcanoes, some still active. The Eastern Cordillera (EC) is the widest, hosting thick Cretaceous to Cenozoic successions, with major coal and hydrocarbon basins shaped by Andean compression. The Western Cordillera (WC), the smallest, is composed largely of accreted oceanic plateau rocks (gabbros, basalts, Cretaceous sediments), and Neogene–Quaternary volcanism. The CC and EC are separated by the Magdalena River Valley, while the CC and WC are separated by the Cauca Valley, both hosting Colombia's main river systems (Figure 3 and Figure 4).

Several foreland and intermontane basins record the tectono-sedimentary evolution of the region. The Middle Magdalena Valley Basin hosts Colombia's oldest giant oil field, La Cira-Infantas, within Cenozoic sediments, with underexplored Cretaceous carbonate targets (ANH, 2010). The Upper Magdalena Basin, a Neogene broken foreland, preserves a Cretaceous to Cenozoic sequence with prolific hydrocarbon reservoirs (Barrero et al., 2007). The Llanos Basin, bounded by the Guaicáramo fault and the Guyana Shield, evolved from Paleozoic rifting into a Maastrichtian—Paleogene foreland basin, now containing over 1700 MMBO of recoverable reserves (ANH, 2010). The Cauca Valley, narrower but strategic, contains volcanic deposits, hydroelectric resources, and a history of gold mining (Figure 4).

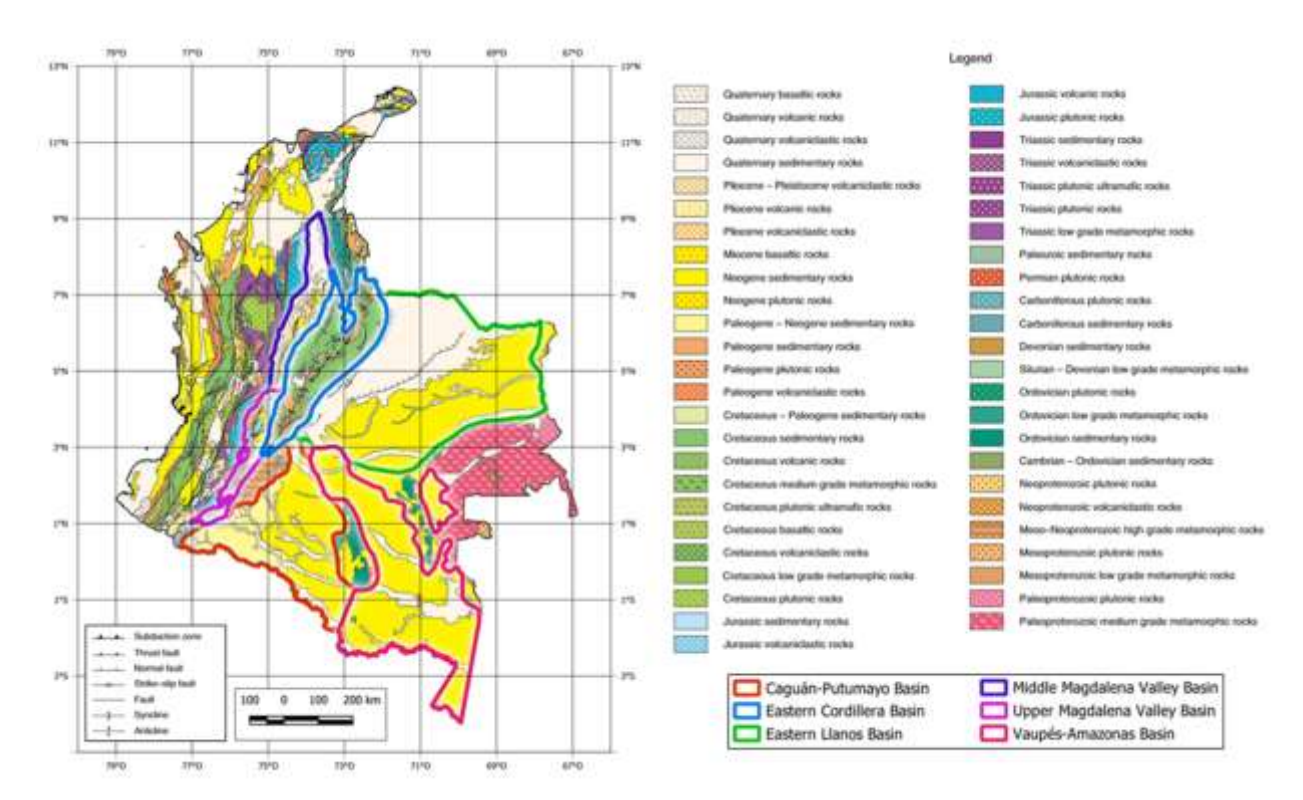


Figure 4. Geological map of Colombia with its main basins, modified from Gómez et al. (2015).

4 Nevado del Ruiz Volcano

The Nevado del Ruiz Volcano (VNR), rising to 5,321 m in the Central Cordillera, is the most studied geothermal area in Colombia and hosts the country's only exploratory well, which reached 1,468 m through seven lithological units and hydrothermal alteration zones associated with high-temperature fluid circulation. Fluid pathways are structurally controlled by faults such as Nereidas, Río Claro, Santa Rosa and Samaná Sur, generating thermal springs with chloride, sulfate, and bicarbonate waters (Aguilera et al., 2019). The western flank, particularly Las Nereidas, Botero-Londoño, El Recodo and Chorro Negro, has been recognized since the 1960s as the most promising geothermal sector (Bona and Coviello, 2016). Currently, five exploratory wells (1,700–2,700 m depth, ~200 °C target) are under environmental assessment.

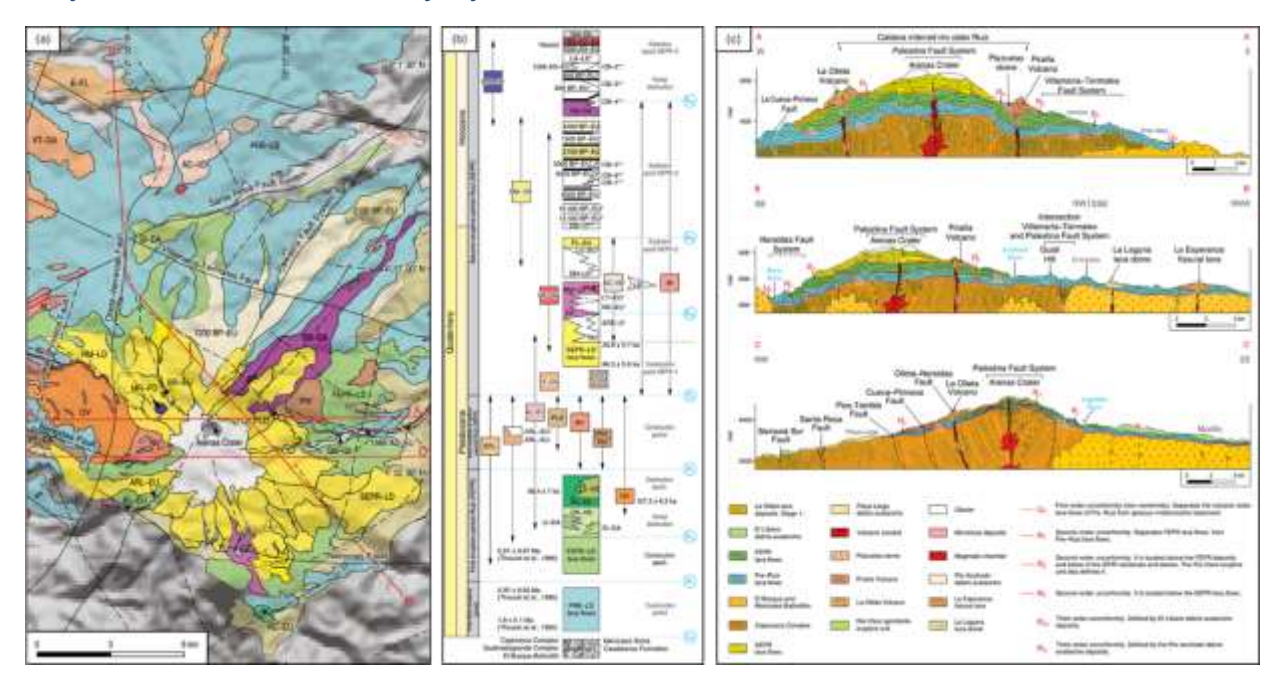
4.1 Geology

The Nevado del Ruiz Volcanic Complex (NRVC) is part of the San Diego–Cerro Machín volcanic–tectonic province of the Central Cordillera of Colombia, located at the convergence of the Nazca, South American, and Caribbean plates (Figure 5). Subduction of the Nazca plate beneath South America, at a velocity of ~55 mm/yr and azimuth of 88°, has controlled the persistence of volcanism in this sector since the Jurassic (Mejía et al., 2014; Ceballos–Hernández et al., 2020). Regionally, deformation is strongly influenced by reactivation of inherited fault systems, including the Palestina, Santa Rosa, Nereidas, Río Claro, and Villamaría–Termales faults, which also act as conduits for hydrothermal circulation (Mejía et al., 2012; Borrero et al., 2009).

The basement of the NRVC is lithologically complex, dominated by the Cajamarca Complex, which includes graphitic schists, quartz—muscovite phyllites, and quartz—amphibole schists (Mejía et al., 2014). To the west of the San Jerónimo Fault, the Quebrada Grande Complex is exposed, while intrusive bodies such as the Manizales Stock (56–57 My; 43.9 My) and the Bosque Batholith (49 My) cut the metamorphic basement (Ceballos—Hernández et al., 2020). Quaternary volcanic deposits unconformably overlie these

units, mainly pyroclastic deposits and lava flows from Cerro Bravo, Santa Isabel, and Nevado del Ruiz volcanoes.

Figure 5. (a) Schematic geological map of the Nevado del Ruiz complex. (b) Litostratigraphic units. (c) Geological cross-sections of the Nevado del Ruiz area (Modified from Ceballos-Hernández et al., 2020).



The eruptive history of the NRVC spans the last 1.8 Ma and has been divided into four main periods (Mejía et al., 2014; Martínez et al., 2014; Rayo and Zuluaga, 2011; Ceballos–Hernández et al., 2020). The Pre-Ruiz stage (1.8–0.97 Ma) produced extensive andesitic lavas (e.g., Gualí, Recreo, El Arbolito). The First Ruiz stage (0.97–0.095 Ma) corresponds to the construction and destruction of the "Older Ruiz," generating ignimbrites (e.g., Río Claro) and partial sector collapse, interpreted as a caldera event. During the Intermediate Ruiz stage (~95–66 ka), satellite edifices such as La Olleta, Piraña, and Nereidas volcanoes developed, with continued activity at La Olleta. Finally, the Second Ruiz stage (66 ka–present) corresponds to the current Nevado del Ruiz stratovolcano. During the last 13 ka, volcanic activity has been predominantly explosive, with at least 14 eruptive events (VEI 2–3), including the 1985 eruption that triggered the Armero tragedy (Thouret et al., 1990; Ceballos–Hernández et al., 2020).

Structurally, several volcanic domes (Laguna, Santana, Plato, Tesorito) align along the Villamaría—Termales fault, highlighting the strong structural control on magmatic emplacement (Borrero et al., 2009). Geochemical analyses classify erupted products as calc-alkaline andesites to dacites, with both high-K and low-K affinities (Schaefer, 1995).

Hydrothermal alteration processes further reveal the interaction between faults and fluids. Forero (2012) identified advanced argillic assemblages in the NW flank, subdivided into acid-sulfate zones restricted to fumarolic vents and silicified zones along fault corridors. The Nereidas geothermal area, bounded by the Palestina, Molinos, and Río Claro faults, is particularly well studied: Paleozoic quartz—graphitic schists, Paleogene dacitic porphyries, and Quaternary ignimbrites are structurally arranged in a graben that channels both magmatic and meteoric fluids (INGEOMINAS, 1997; Martínez et al., 2014).

This integrated geological framework, combining stratigraphic, tectonic, volcanic, and hydrothermal data, positions the NRVC as Colombia's best-characterized geothermal prospect. It also provides the foundation for geophysical modeling and reservoir capacity estimates that are discussed in subsequent sections (Mejía et al., 2014; Moreno et al., 2018).

4.2 Geochemistry of Hydrothermal Fluids

Numerous geochemical studies have addressed the hydrothermal system of the Nevado del Ruiz Volcano (VNR), both academic and applied, providing key information for geothermal exploration.

Early investigations by López (1992) classified five water types in the VNR hydrothermal system (dilute acidic, dilute bicarbonate, acidic sulfate brackish, bicarbonate brackish, and neutral chloride brackish waters) using the Giggenbach scheme. Neutral chloride waters dominate the western flank, acidic sulfate waters align with the Villamaría—Termales and Palestina faults, and bicarbonate waters are more dispersed. López emphasized that VNR waters are not in equilibrium, representing intermediate stages of rock—water interaction.

Partida et al. (1997) analyzed geothermal manifestations on the eastern flank (Río Claro–Las Nereidas), concluding that VNR reflects a shallow acidic magmatic chamber. They distinguished two fluid circulation systems: sulfate waters to the north and neutral chloride waters to the west. Geothermometry indicated reservoir temperatures of ~235 °C, supported by Na–K–Ca, Na/K, and Cation Composition Geothermometer (CCG) indices, although Mg-corrected values underestimated temperatures. Key springs include Botero Londoño and La Piscina (chloride–sodium, geothermal), and Las Nereidas (sulfate, Ca–bicarbonate) (Table 1). Structural control by the Río Claro and Las Nereidas faults was identified.

Table 1. Geothermometric results for the studied springs (Botero Londoño and La Piscina). Values show good agreement between Na-K-Ca, Na/K and TCCG geothermometers, while the magnesium-corrected geothermometer yields underestimated values. Data from Partida et al. (1997).

Spring		TNaKCa (°C)	TNa/K (°C)	TCCG (°C)	Note
B1 Londoño)	(Botero	210–235	239–267	225–255	Good agreement
B2 Londoño)	(Botero	211–236	241–272	227–258	Good agreement
LP (La Piscina)		148-314	243–423	168–241	Wider spread; Mg-corrected values very low

Subsequent studies reinforced these findings. Correal (2013) described a circulation system of bicarbonate—alkaline waters with low salinity, linked to meteoric recharge interacting with silicate-rich basement rocks. Interaction with CO_2 -enriched gases along permeable faults increases salinity without altering other compositional traits. Gas geochemistry showed CO_2 – N_2 dominated mixtures, with H_2 as an indicator of high-temperature zones, and geothermometers suggested reservoir temperatures near 209 °C.

Federico et al. (2017), analyzing steam discharges during recent volcanic activity, reported δ¹8O shifts in Agua Caliente and Botero Londoño, indicating isotopic exchange with magmatic fluids. Their estimates suggest deeper reservoir temperatures of ~315 °C, higher than previous geothermometric results, highlighting heterogeneity in the hydrothermal system.

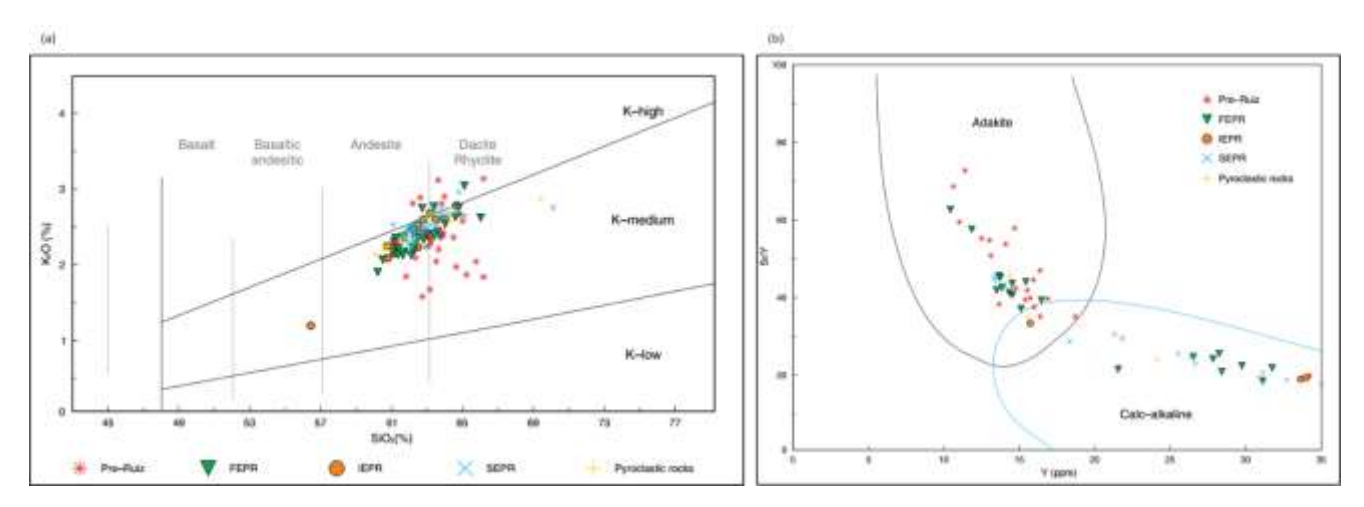
Collectively, these studies converge on the existence of a mixed magmatic-meteoric hydrothermal system at VNR, structurally controlled by major faults. Reservoir temperatures range from ~200 to 315 °C depending on methodology and sampling site, confirming the geothermal potential of the Nereidas and Botero Londoño areas.

More recently, Ceballos–Hernández et al. (2020) presented a comprehensive geochemical synthesis of the NRVC volcanic products, showing compositions ranging from basaltic andesites to dacites with typical

calc–alkaline affinities. Their major- and trace-element analyses highlight fractional crystallization, subduction-related enrichment in LILEs, and crustal assimilation as key processes. Importantly, several eruptive units display an adakitic geochemical signature (high Sr, low Y and Yb, high Sr/Y ratios), consistent with the subduction of young oceanic lithosphere beneath the Central Cordillera. These magmatic characteristics provide the thermal and geochemical context for the high-temperature hydrothermal system identified in the western flank of the volcano.

Representative samples from the NRVC range from basaltic andesites to dacites with medium- to high-K calc–alkaline affinity (Figure 17). Trace-element ratios also reveal adaktic signatures in several eruptive units, expressed as high Sr/Y and low Y and Yb values, consistent with magma derivation from young, subducted lithosphere (Figure 6) (Ceballos–Hernández et al., 2020).

Figure 6. Geochemical diagrams of the Nevado del Ruiz Volcanic Complex (NRVC): (a) SiO_2-K_2O classification showing medium- to high-K calc-alkaline compositions; (b) Sr/Y-Y diagram evidencing adakitic signatures in several eruptive units. Taken from (Ceballos-Hernández et al., 2020).



Overall, the integration of hydrothermal fluid studies and volcanic product geochemistry supports the presence of a high-temperature geothermal system in the western flank of the NRVC, controlled by fault structures and sustained by a magmatic heat source with adaktic affinities (López, 1992; Partida et al., 1997; Correal, 2013; Federico et al., 2017; Ceballos–Hernández et al., 2020).

4.3 Hydrothermal Alterations

Hydrothermal alteration at the Nevado del Ruiz Volcano (VNR) results from the interaction of magmatic and meteoric fluids with the volcanic basement. Forero (2012) characterized in detail the NW flank using isotopic and petrographic analyses, identifying the influence of gases in generating alteration restricted to older lava flows. Two main subsets were described: acid—sulfate alteration, localized near fumarolic vents, and silicification, concentrated along fault zones.

The most significant regional expression is an advanced argillic alteration, with assemblages of quartz, kaolinite, illite, smectite, amorphous clays, and sulfates. Both acid–sulfate alteration and silicification represent subgroups of this argillic alteration. δ^{18} O results suggest an important magmatic component in their genesis (Forero, 2012).

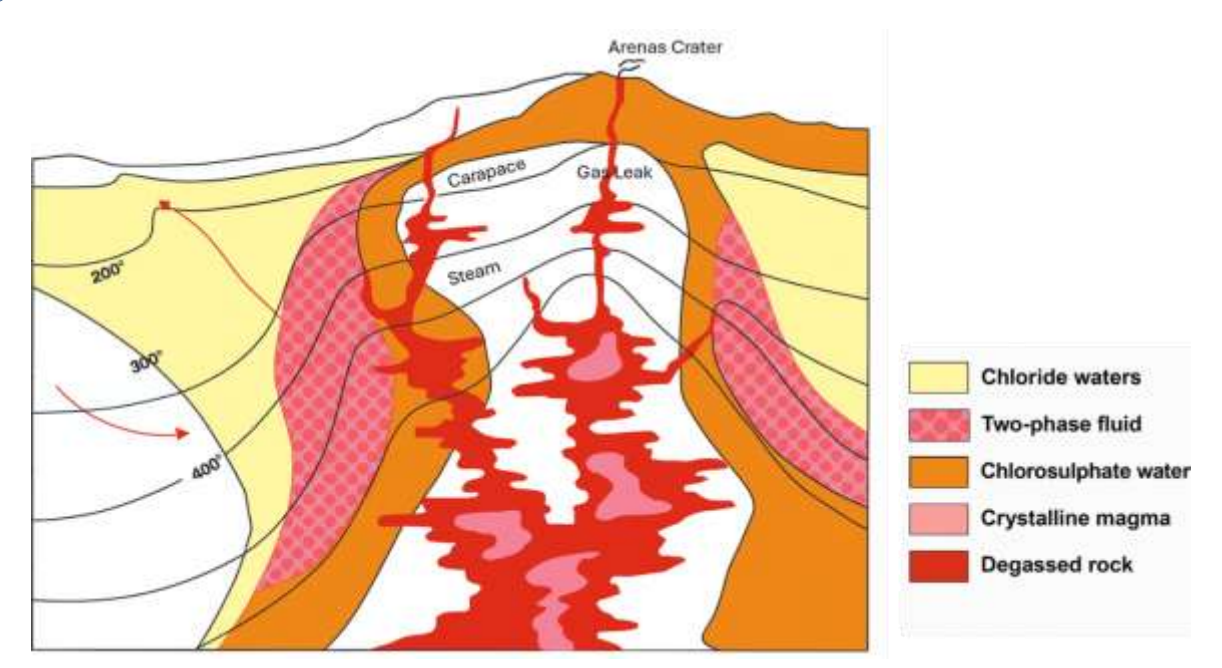
Spatial variability reflects multiple hydrothermal systems. In Santa Rosa and Hacienda El Termal, neutral CO₂-rich fluids precipitate amorphous silica and carbonates, whereas in the northern sector acidic thermal waters precipitate sulfates. The Nereidas vent, near the Olleta volcano, shows restricted steamheated alteration affecting only colluvial deposits around fractures.

Fault systems exert major control. Along the Villamaría–Termales fault, silicification reflects the ascent of acidic fluids >150 °C in a magmatic–hydrothermal setting, but also lower-temperature silica polymorphs (chalcedony, opal, tridymite) indicate meteoric inputs. On the Palestina fault, advanced argillic alteration is more intense, associated with both meteoric fluids and magmatic vapors, supporting the acidification of neutral waters.

Finally, unaltered lava flows overlying altered zones indicate an ancestral alteration event of long duration. Low δ^{34} S values reinforce this interpretation, confirming sustained magmatic fluid–rock interaction (Forero, 2012) (Figure 7).

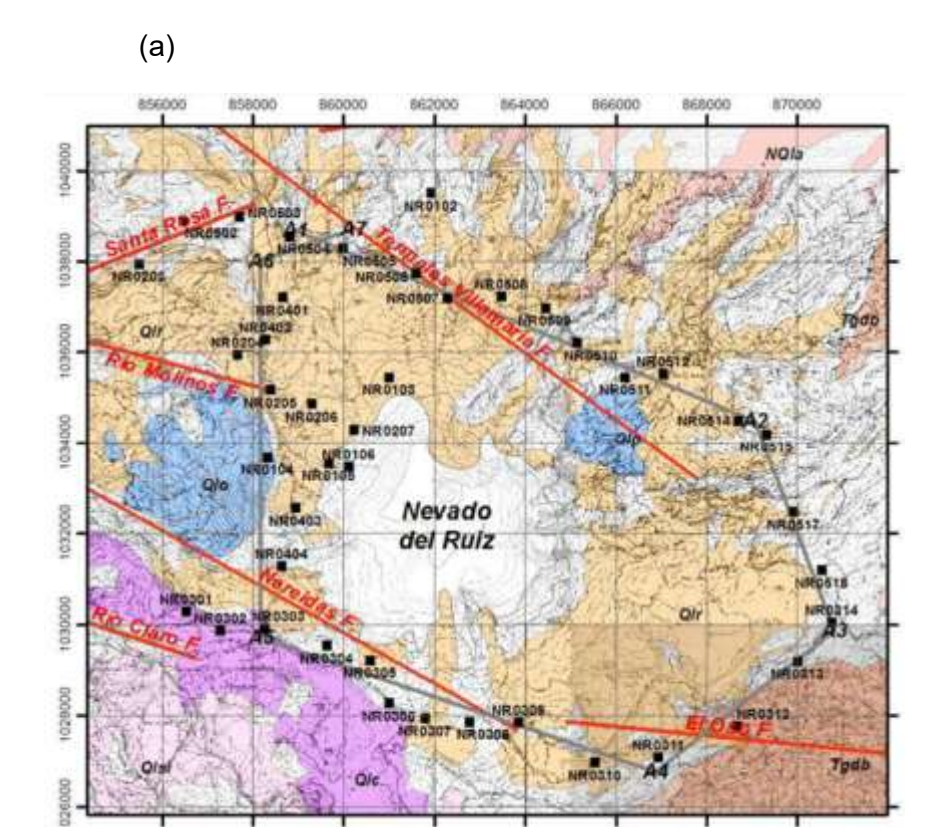
Earlier work by López (1992) identified mineral assemblages consistent with the two main hydrothermal water types at VNR. Acid–sulfate waters were associated with cristobalite, sulfates, pyrite or hematite, and minor tridymite, kaolinite, smectite, and illite, while neutral chloride and bicarbonate waters produced carbonate minerals (dolomite, calcite, siderite) and cristobalite, with gypsum and halite as evaporation products. These results corroborate the link between fluid chemistry and alteration parageneses, later refined by isotopic and petrographic analyses (Forero, 2012).

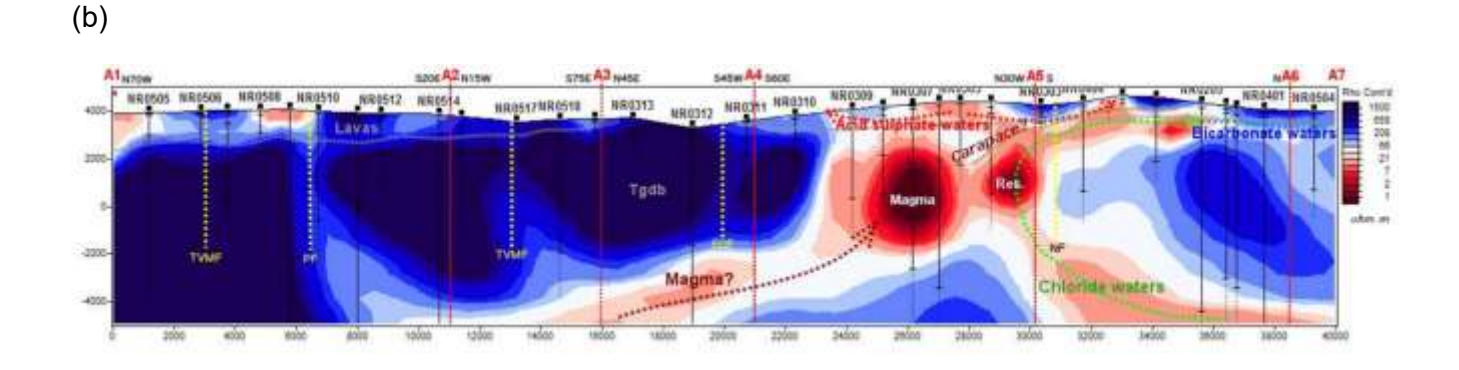
Figure 7. Conceptual model of the Nevado del Ruiz hydrothermal system, summarizing the spatial distribution of chloride, acid-sulfate, and two-phase fluids in relation to the magmatic body and structural conduits, based on Lopez (1992) and Forero (2012) works.



Hydrothermal alteration patterns described by López (1992) and Forero (2012) are consistent with resistivity anomalies imaged by González-García et al. (2015), where MT sections delineate low-resistivity zones spatially correlated with chloride-, sulfate-, and bicarbonate-rich waters (Figure 8). These results reinforce the structural and geochemical evidence of multiple hydrothermal systems within the NRVC.

Figure 8. Magnetotelluric survey around the Nevado del Ruiz Volcanic Complex (NRVC). (a) Perimetric MT survey lines across major fault systems (Santa Rosa, Villamaría—Termales, Río Molinos, Río Claro). (b) Resistivity profile showing low-resistivity anomalies associated with hydrothermal fluids, spatially correlated with chloride, acid-sulfate, and bicarbonate waters. Modified from González-García et al. (2015).





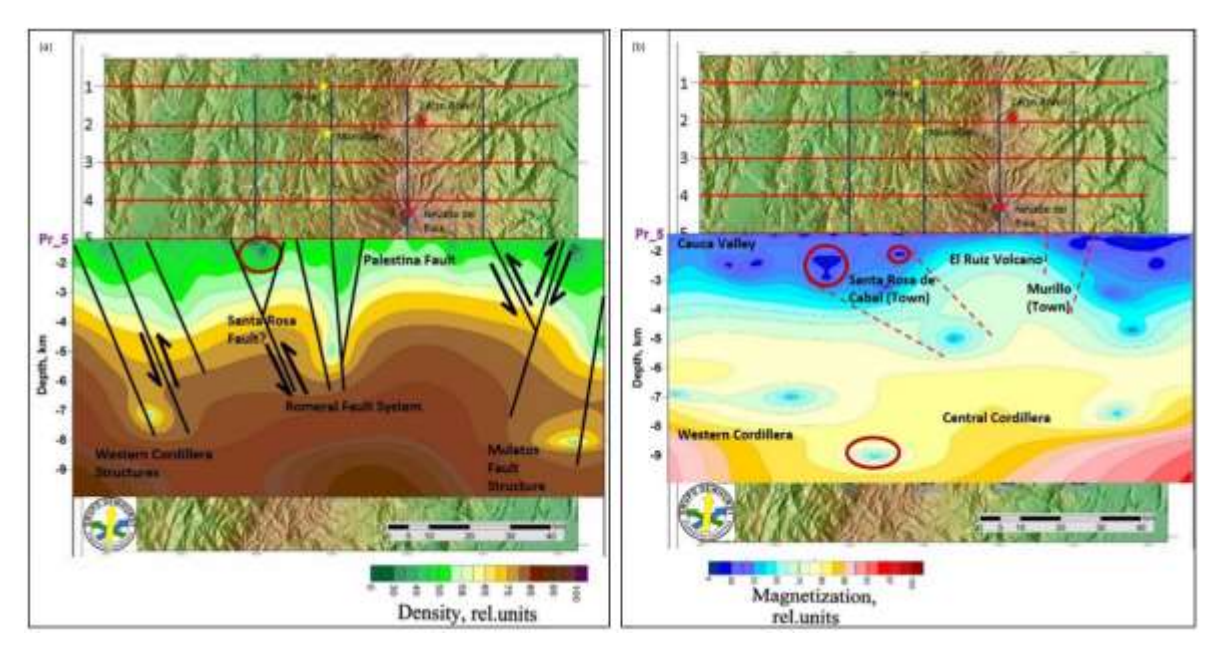
4.4 Geophysical Analyses

Geophysical methods provide indirect insights into subsurface structures relevant for geothermal exploration. At the Nevado del Ruiz Volcano (VNR), surveys have combined gravimetry, magnetometry, magnetotellurics (MT) (Figure 8), and thermal modeling.

During the pre-feasibility stage, ISAGEN conducted multidisciplinary studies supported by Colciencias (Marzolf, 2014). Magnetotelluric soundings processed by Sarmiento (2014) produced 1D–2D resistivity models that identified a deep conductive body to the SE, a large resistive structure to the NW, and shallow high-conductivity zones in the central sector. Vargas and Dewhurst (2014), integrating gravimetry and

MT with GIS, confirmed structural controls in the Las Nereidas area, delineating low-resistivity pathways that enhance geothermal potential. Their results are summarized in density and magnetization models (Figure 9), which highlight the influence of major fault systems such as Palestina, Santa Rosa, Romeral and Mulatos in controlling deep anomalies and potential fluid pathways. It's important to highlight the importance of stratigraphic and structural heterogeneity in the Cajamarca and Quebrada Grande complexes, which complicates MT interpretations due to mixed conductive and resistive lithologies (García et al., 2013).

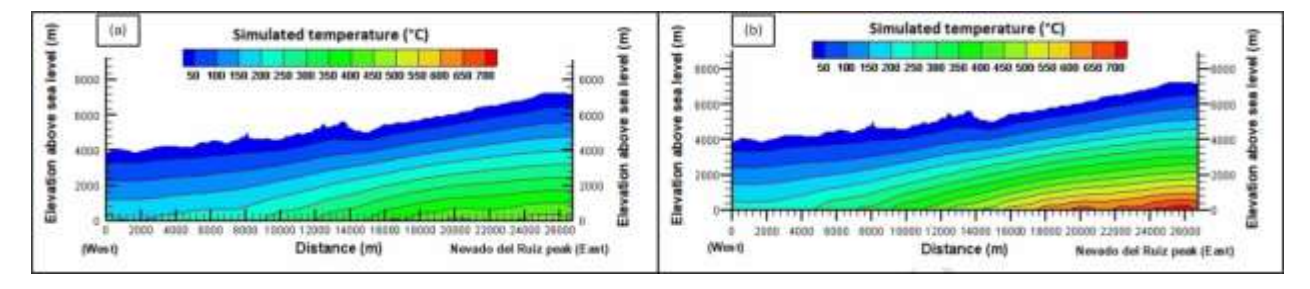
Figure 9. Geophysical models across the Nevado del Ruiz Volcanic Complex (NRVC) showing (a) density and (b) magnetization anomalies. The sections illustrate the structural influence of the Palestina, Santa Rosa, Romeral, and Mulatos faults, and highlight low resistivity/magnetic zones that may represent preferential fluid pathways. Taken from Vargas & Dewhurst (2014).



Subsequent modeling advanced resource quantification. Vélez et al. (2017) incorporated rock thermal conductivity into heat-transfer simulations of the Cajamarca Complex. Two scenarios were tested: (a) constant conductivity and (b) temperature-dependent conductivity. Both exceeded 200 °C at depth, but scenario (b) proved more realistic.

The simulated temperature profiles for both scenarios are shown in Figure 10, highlighting the influence of conductivity assumptions on subsurface temperature estimations. Estimated capacity was 30–40 MWe, consistent with Mejía et al. (2014). The study emphasized the need for detailed fieldwork and fault characterization to refine models.

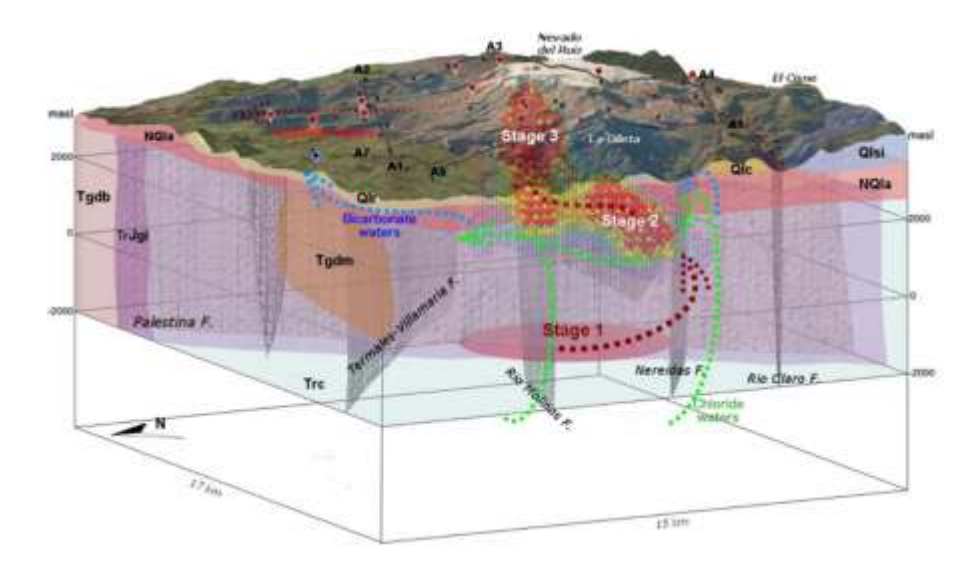
Figure 10 Simulated temperature profiles across the Nevado del Ruiz Volcanic Complex based on heat-transfer modeling of the Cajamarca Complex (Vélez et al., 2017). (a) Scenario with constant thermal conductivity; (b) scenario with temperature-dependent conductivity.



Building on these results, Moreno et al. (2018) evaluated the effect of fault dip on fluid and heat transport along the Samaná Sur fault, which crosses the geothermal reservoir. Three scenarios were considered: dip 8°SE, 45°SE, and 80°SW. Results showed that dips favoring groundwater flow increased simulated surface temperatures, whereas opposing dips reduced them. This analysis confirmed fault geometry as a critical factor in reservoir behavior and underscored the need for improved estimates of hydraulic conductivity to strengthen predictive models.

González-García et al. (2015) built a three-dimensional conceptual model derived from MT data and seismogenic zones that summarizes the hydrothermal architecture of the NRVC (Figure 11). It highlights the role of major faults, such as Palestina, Villamaría–Termales, Nereidas, and Río Claro, in channeling chloride, sulfate, and bicarbonate waters, and delineates three hydrothermal stages connected to the magmatic heat source. This integrated view reinforces the geophysical evidence of a structurally controlled, multi-fluid geothermal system.

Figure 11. Three-dimensional conceptual model of the Nevado del Ruiz Volcanic Complex integrating MT data and seismogenic zones. Taken from González-García et al. (2015).



Together, these geophysical investigations converge on a model where conductive anomalies, structurally controlled pathways, and heterogeneous thermal properties govern the geothermal potential of the VNR, supporting capacity estimates of ~30–50 MWe (Vélez et al., 2017; Moreno et al., 2018).

More recent assessments by Alfaro et al. (2020) quantified stored heat and potential generation capacity for specific geothermal clusters. Their results indicate that Nereidas—Botero Londoño concentrates the highest potential, with a mean of ~12 EJ of stored heat and ~100 MWe of electrical capacity, followed by Hacienda Granates (~11.6 EJ; ~67 MWe), and Villamaría—Termales (~4.8 EJ; ~39 MWe). Despite methodological uncertainties, these values reinforce the strategic importance of the western flank of the NRVC and highlight the variability between neighboring systems. Collectively, the integration of geological, geochemical, and geophysical data positions the Nevado del Ruiz as Colombia's best-characterized geothermal prospect, with realistic potential in the order of tens to hundreds of megawatts depending on the sector considered.

5 Azufral Volcano

The Azufral geothermal area is located in the Western Cordillera of southwestern Colombia (Department of Nariño), ~25 km north of the border with Ecuador. The town of Túquerres lies at the eastern base of the volcanic edifice, and the site is strategically close (~25 km) to the 220 kV Colombia–Ecuador interconnection line (Bona and Coviello, 2016).

The area was first classified as a high-priority geothermal prospect in 1982. However, systematic investigations began in the late 1990s under the direction of INGEOMINAS, with support from the Inter-American Development Bank (IDB) and financing from the Japan Trust Fund. In 2001, a pre-feasibility study was awarded to West Japan Engineering Consultants and Geohazards Consultants International, but the project was cancelled in 2002 due to security issues and lack of local support. INGEOMINAS subsequently continued the work, completing geological mapping in 2003 and conducting geothermal exploration in 2006 (Ovalle, 2020).

Multidisciplinary studies—including structural geology, gravimetry, magnetometry, geoelectrics, hydrothermal alteration mapping, fluid geochemistry, and conceptual modeling—indicate that the Azufral hydrothermal system reaches subsurface temperatures of ~225 °C (Alfaro et al., 2008). Surface manifestations (hot springs, fumaroles, alteration zones) are mainly controlled by fault systems and their intersections (Aguilera et al., 2019). Azufral is considered one of Colombia's most explosive volcanoes and remains active, with persistent hydrothermal and fumarolic activity (Torres et al., 2001).

Most recently, Ecopetrol obtained an exploration permit and initiated a geothermal exploration project at Azufral in 2025, marking a significant step toward the development of high-enthalpy resources in the country (Ecopetrol, 2025).

5.1 Geological Setting

Azufral Volcano is located in the Western Cordillera, in the department of Nariño, 30 km SW of the city of Pasto and 30 km north of the Colombian-Ecuadorian border, on what is called the Northern Volcanic Zone of the Andes (NVZ), which extends from Ecuador to the northern part of Colombia, forming volcanic belts oriented north-south (Rangel, 2017).

The Western Cordillera is built on a Mesozoic allochthonous metamorphic basement, formed by oceanic affinity metavolcanic rocks such as phyllites, shales and shales of sedimentary protolith, and marine sedimentary rocks of very fine grain size such as shales, siltstones and mudstones; and it is mainly constituted by volcanic and sedimentary rocks of Cretaceous age that have been divided into two main groups: the Diabassic Complex, of Coniacian-Turnonian age and composed of massive basaltic rocks or in pillow lavas, with microgabbros and tuffaceous intercalations with sedimentary rocks; and the Dagua Complex, of Lower to Upper Cretaceous age and constituted by marine sedimentary rocks with volcanic intercalations affected by dynamic and local metamorphism, divided into the following groups in the Espinal and Cisneros formations of Albian to Maastrichtian age (Gonzalez et al., 2002; Rangel, 2017).

Both groups have been intruded by intermediate plutonic bodies (andesites to quartzodiorites) of Paleogene-Neogene age and by andesitic to dacitic bodies related to the Piedrancha batholith (Gonzalez et al., 2002) (Figure 12). All these units are covered by ignimbritic, laharic and pyroclastic deposits of Neogene and Holocene age.

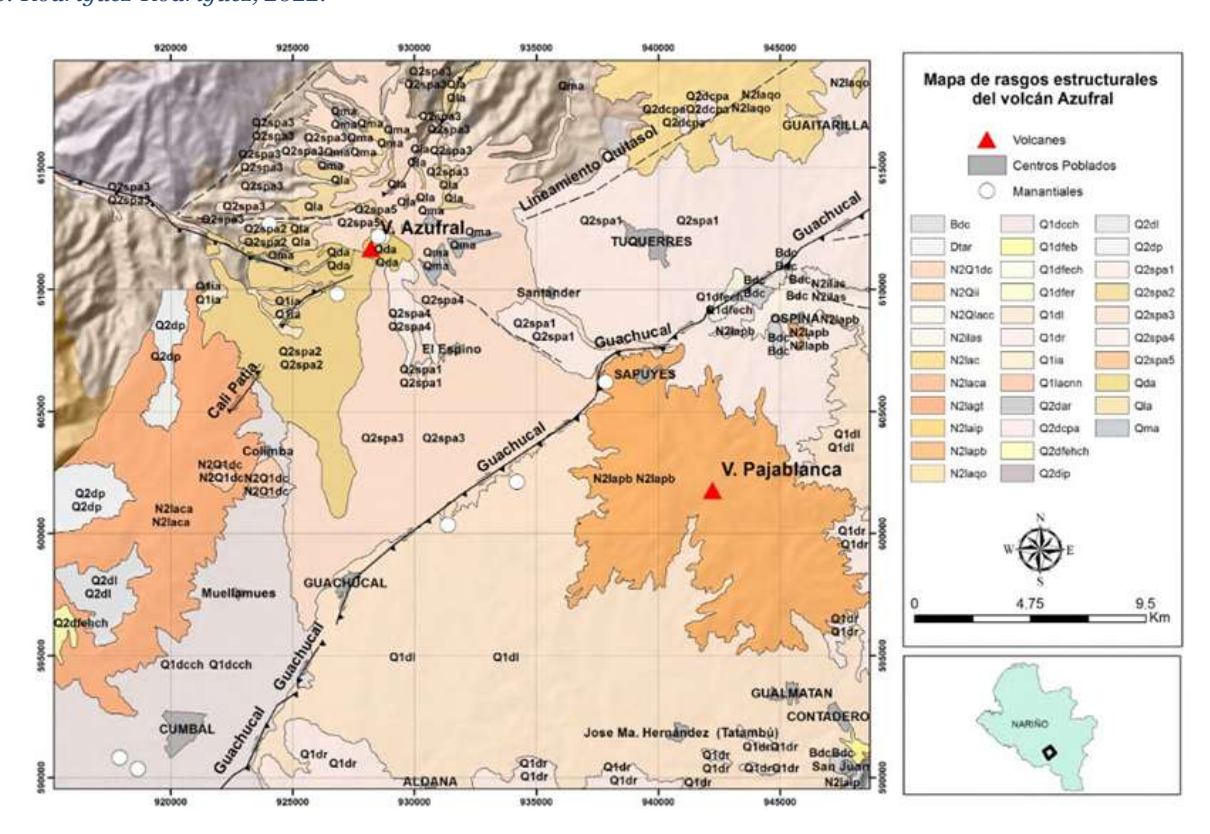


Figure 12. Geological map of the Azufral Volcano region, mostly covered by Quaternary deposits and Neogene formations, source: Rodríguez-Rodríguez, 2022.

The current volcanic edifice of Azufral is built on Cretaceous rocks, ultramafic and mafic plutonic, basic volcanic and metasedimentary, the latter belonging to the Dagua Structural Complex and all grouped in the so-called Western Cretaceous Oceanic Lithospheric Province (PLOCO), which constitute the base of the Western Cordillera and the Cauca- Patía inter-cordilleran depression. Intruding these rocks are Paleogene and Neogene igneous bodies and discordantly covering all the previous rocks, there are deposits and effusive, explosive and extrusive rocks of the Neogene and Quaternary, affected by faults of the Cali-Patía system, located towards the eastern foothills of the Western Cordillera (Torres et al., 2001).

The map of volcanic hazards and risks of Azufral Volcano prepared by INGEOMINAS in 2001 defined the geology and stratigraphy of the Neogene and Quaternary deposits and identified eight eruptions of dacitic composition represented by sequences of pyroclastic flows of ash and blocks, ash and pumice, and pyroclastic surges, the latter with a wide distribution in the area and considerable thickness. This leads to the conclusion that the recent activity of the Azufral stratovolcano has been highly explosive. The ancient sequences are made up of ignimbrite deposits and andesitic lavas, the latter dating to 0.58±0.03 Ma (Torres et al., 2001). Azufral volcano does not present glaciers and its edifice highlights the general presence of deposits associated with lava flows, large pyroclastic flows and pyroclastic fall deposits (Rangel, 2017).

The Azufral volcano responds tectonically to the subduction of the Nazca plate under the South American plate, a phenomenon that causes a complex structural style in the Western Cordillera, presenting a predominant occurrence of high-angle strike-slip faults with N-NE direction (González et al., 2002). This trend, which has been characterized by a series of active and potentially active faults parallel to the Romeral fault system, has been related to the collision of the previously mentioned plates (Nazca-South American) during the Cretaceous. This group of faults is known as the Cauca-Patía Fault System, which dips constantly to the east with angles between 50° and 70° and is located in the depression between the Eastern and Central Cordilleras towards the southeast of the country (Rangel, 2017).

To the east, the study area is bounded by the Silvia-Pijao fault, described as a north-south trending fault with a dip plane to the east. Additionally, the presence of perpendicularly oriented lineaments has also been reported, oriented to the NW, which are related to transverse faults and seem to correspond to ancient basement faults (González et al., 2002; Rangel, 2017). The faulted structures are mostly covered by volcanoclastic deposits.

Faulting, layering and shearing present NE-SW predominance, and two main fracture directions are distinguished: NE-SW and NW-SE (Gonzalez et al., 2002), which is important in terms of geothermal fluid migration (Rangel, 2017). The important aspects to consider about Azufral Volcano as a potential geothermal resource are its recent age and persistent volcanic activity, the complete magmatic evolution and differentiation (from andesites to rhyodacites), the presence of superficial thermal manifestations, and the superficial hydrothermal alteration (argillic, phyllic and propylitic), which will be discussed later.

5.2 Fluid Geochemistry

Preliminary geochemical studies at the Azufral Volcano were conducted within the INGEOMINAS Groundwater Exploration Program (PEXAS), focusing on thermal waters and steam vents. These analyses revealed a distribution compatible with geothermal systems of stratovolcanoes, with evidence of reservoir fluid mixing with salinized waters (Alfaro et al., 2008). Geothermometric data suggested reservoir temperatures between 240 and 480 °C, supporting the classification of Azufral as a high-enthalpy geothermal system (Table 2).

 $Table\ 2.\ Estimated\ temperatures\ for\ the\ Azufral\ Volcano\ geothermal\ reservoir\ (two\ different\ intakes), from\ geothermometers.$ $Taken\ from\ Alfaro\ et\ al.,\ 2008.$

Geothermometer	T °C	T2 °C
H₂/Ar	360	371
CO ₂ /Ar	319	319
CO ₂ -H ₂ S-CH ₂ -H ₄	407	423
CH ₄ /CO ₂	430	417
CO ₂	406	419
CO-CO ₂ -CH ₄	283	252
CO ₂ /H ₂	239	248
δ^{13} C (‰) CH ₄ /CO ₂	955	629
δ^{13} C (‰) CH ₄ /CO ₂	836	541

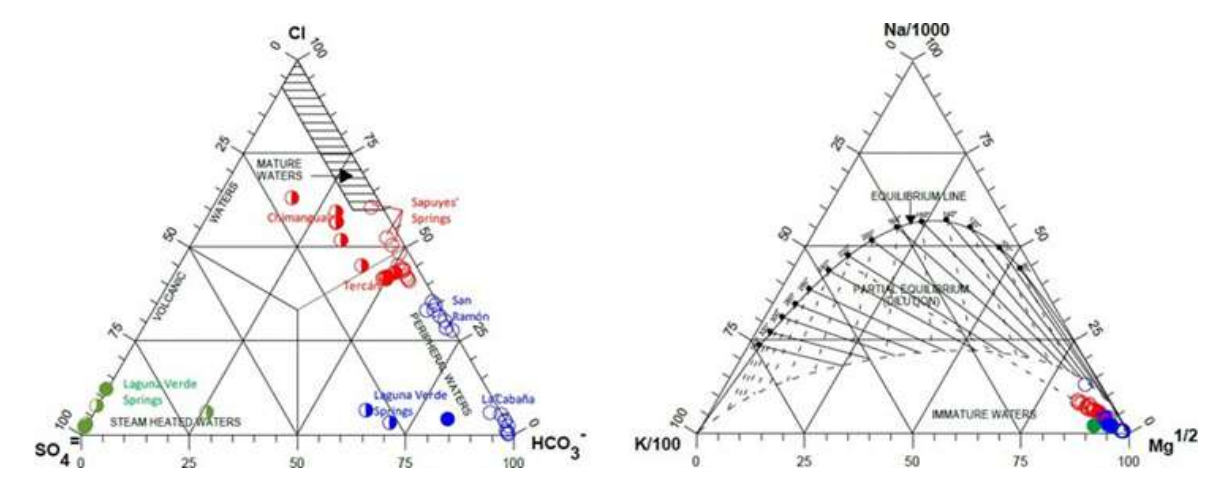
Subsequent work by Rangel (2017) provided a detailed compositional analysis of springs, grouping thermal waters into four main types: (i) moderately acidic to neutral sulfate springs, (ii) sodium chloride waters of moderate to high temperature, (iii) chloride—sodium waters with significant bicarbonate concentrations, and (iv) low-temperature magnesium bicarbonate waters, the latter interpreted as

meteoric. These categories were linked to surface origin, deep geothermal waters, mixing processes, and meteoric end-members, respectively. Reservoir temperatures were estimated at 179–208 °C, with Na–K geothermometers providing the most consistent values (~180–210 °C). This study reinforced the potential for both direct uses (balneology, agriculture, heating) and electricity generation.

A more integrative conceptual model was presented by Alfaro et al. (2015), defining four main discharge areas—Crater, Tercán, Chimangual, and Sapuyes—plus isolated springs at San Ramón and La Cabaña. These manifestations are structurally controlled by the Carbán, Chimangual, Cali—Patía, Azufral—Sapuyes, and Chimangual faults. In the Giggenbach and Goguel (1991) diagram, crater fluids plot as acid sulfate and bicarbonate—sulfate mixtures, Chimangual as neutral chloride, Tercán and Sapuyes as neutral chloride with bicarbonate, and San Ramón—La Cabaña as neutral bicarbonate (Figure 13).

Geothermometry confirms high subsurface temperatures. Aqueous geothermometers yield ~180 °C (quartz) to 250 °C (Na/K) (Figure 13), while gas geothermometers from vents (85 °C discharge) estimate 190–300 °C (Alfaro et al., 2015). These results converge on a reservoir of at least 200 °C, aligning with high-enthalpy geothermal potential.

Figure 13. Relative chemical composition of Azufral volcano hot springs. The Na/K geothermometer indicates a probable reservoir temperature of at least 200 °C. Taken from Alfaro et al., 2015.



5.3 Hydrothermal Alterations

As part of the geological, seismic and geothermal research project in the Altiplano Nariñense, carried out jointly by INGEOMINAS and the National University of Colombia, within the framework of the INGEOMINAS groundwater exploration program (PEXAS), the mapping of surface hydrothermal alteration was carried out based on sampling and analysis of fresh and altered rocks. The study, based on surface alteration, allowed establishing a vertical zoning identifying advanced argillic, argillic, phyllic and propylitic zones. Quartz fillings and other forms of silica filling open fractures with NW - SE direction are also recognized. The vertical zonation has been previously established from the study of lithics collected in a pyroclastic deposit in the Espino area in the study of Recognition of the geothermal resources of the Republic of Colombia.

The preliminary conceptual model based on surface hydrothermal alteration allows inferring a mature high-temperature geothermal system with a magmatic heat source located mainly to the east of the volcano, which is consistent with the geochemical model based on the distribution and characterization

of surface manifestations (hot springs and fumaroles) of Azufral Volcano. An upward flow cuts the surface towards the northeast of the crater, where a boiling process is recorded, evident in the existence of advanced argillic alteration, formed by steam-heated fluids, which develop in a surface environment characterized by the oxidation of H_2S (Figure 14) (Carvajal et al., 2008). This process is consistent with that defined in the geochemical characterization of hot springs (Alfaro et al., 2008).

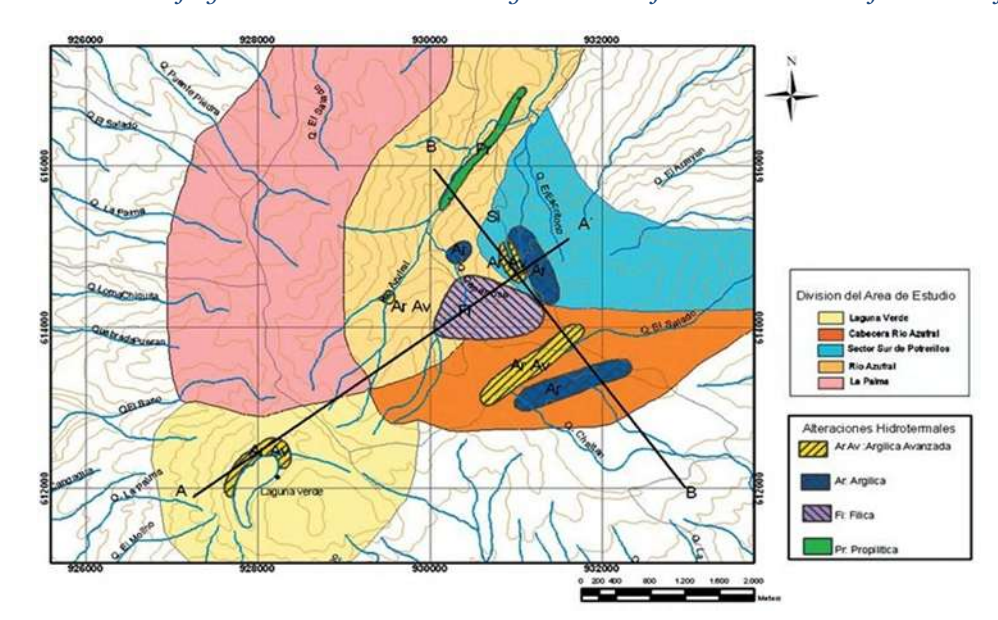


Figure 14. Spatial distribution of hydrothermal alteration recognized at Azufral Volcano. Taken from Carvajal et al., 2008.

The remaining mineral associations related to argillic, phyllic and propylitic alteration zones, located from higher to lower elevations, highlight the vertical zonation characteristic of mature geothermal systems developed in andesitic stratovolcanics (Carvajal et al., 2008). The estimate from both geothermometers and well-developed vertical zonation of hydrothermal alterations is for the reservoir temperature is between 250 and 280°C and would be located in a propylitic zone in the sequence of andesitic lavas or volcano-sedimentary rocks (argillites and siltites) (Alfaro et al., 2015).

5.4 Geophysics

Early potential-field studies by Ponce (2013) identified subsurface anomalies at Azufral characterized by low density and very low magnetic susceptibility, interpreted as the result of elevated temperatures and hydrothermal alteration. Areas with high gravity but low magnetization suggested altered igneous rocks and pyroclastic deposits. From these data, geothermal gradients of 150–250 °C/km were estimated, implying a medium- to high-temperature reservoir (<2 km depth) with ~242 °C at fault-controlled zones, consistent with magma ascent pathways.

Subsequent integrated surveys by the Colombian Geological Survey expanded this framework through regional and residual anomaly mapping (Alfaro et al., 2015). Curie-point depth estimates ranged from 2.3 to 14.2 km, with a geothermal gradient of 121 °C/km below the volcanic edifice and a Curie depth of ~4 km. Gravimetric and magnetic anomalies delineated favorable sectors west of Túquerres (Figure 15).

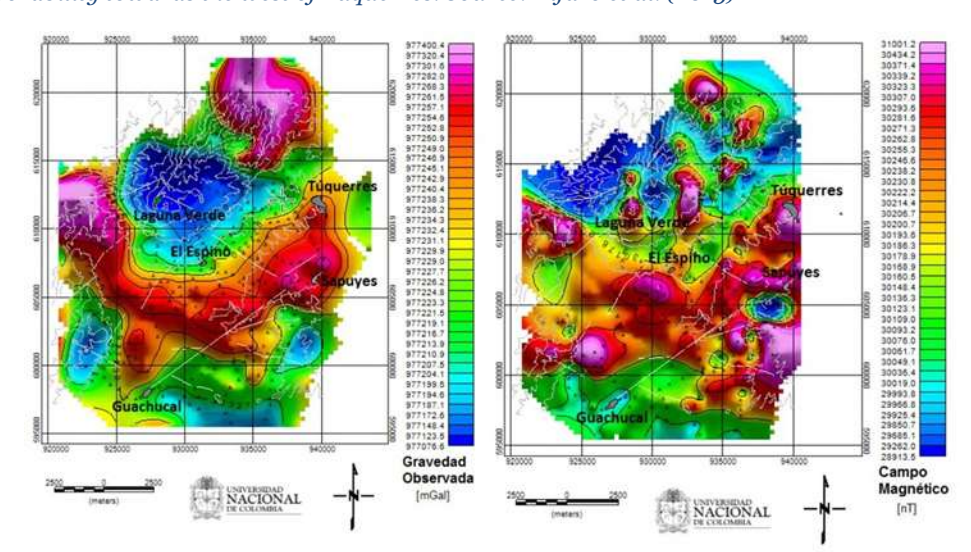


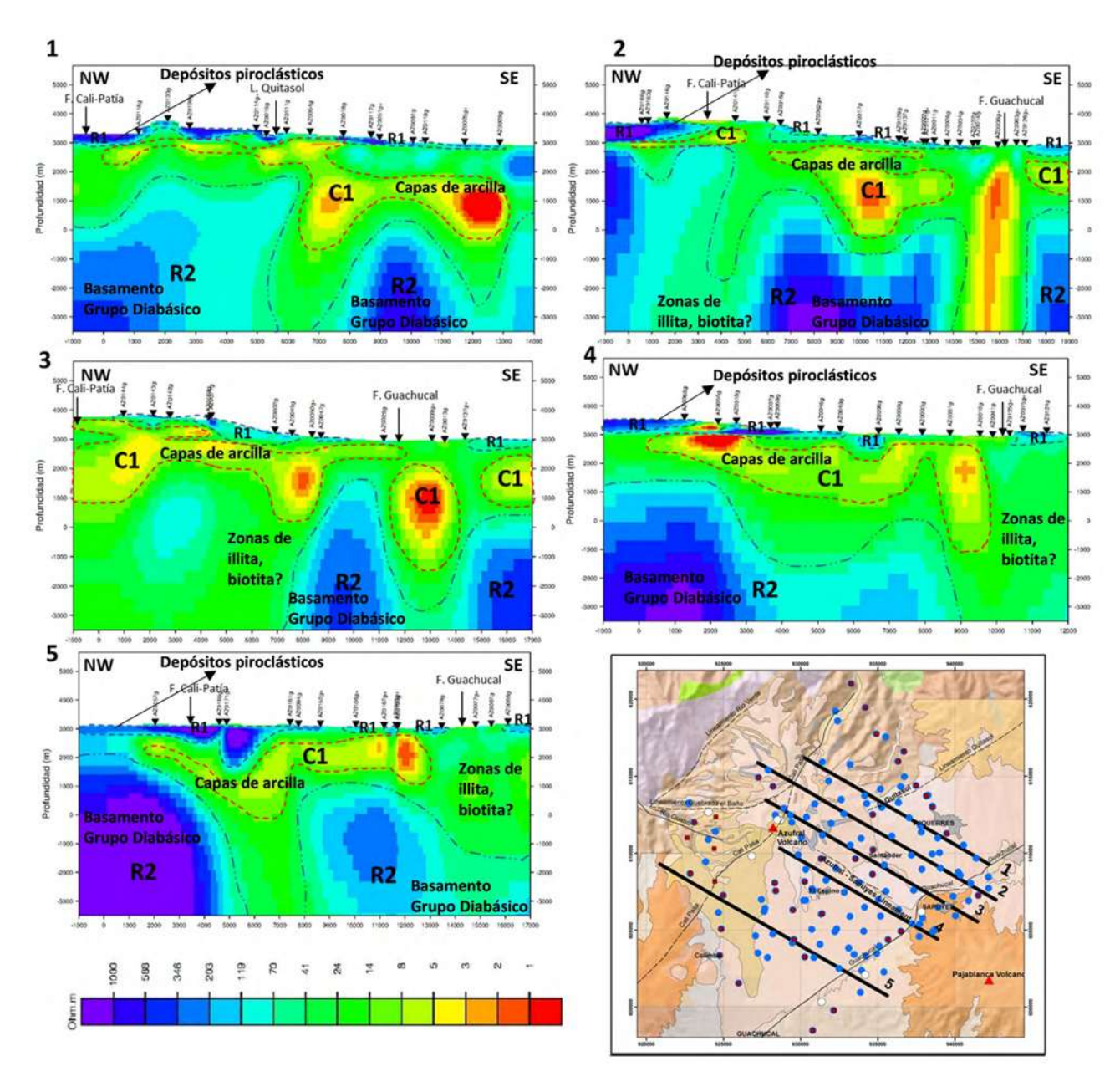
Figure 15. Gravimetric and magnetic model of the Azufral Volcano area, low gravity and magnetic anomalies were found, which defines favorability towards the west of Tuquerres. Source: Alfaro et al. (2015)

These results were complemented by geoelectric and seismological studies, which confirmed structural controls favorable for fluid storage and circulation. The main accumulation zone is bounded by the El Diviso–Túquerres fault (north–south), the Muellamués fault (west), and the Guachacal fault (east), with hydrothermal circulation preferentially following NW–SE faults such as Azufral–Sapuyes (Alfaro et al., 2015). Low permeability to the west of the edifice restricts fluid migration, further concentrating resources in this structurally defined compartment.

More recently, Rodríguez-Rodríguez (2023) applied 2D magnetotelluric (MT) modeling supported by 140 MT and 39 TDEM stations, providing the most detailed resistivity framework for Azufral to date. The models delineate three main domains: (i) shallow resistive anomalies ($\geq 100~\Omega \cdot m$) corresponding to unaltered pyroclastic deposits; (ii) a laterally continuous conductive layer ($\leq 2~\Omega \cdot m$, ~1.2 km thick) interpreted as a clay-rich cap sealing the geothermal system; and (iii) deeper resistive bodies ($> 100~\Omega \cdot m$) attributed to the Diabasic Group basement. Intermediate anomalies ($10-100~\Omega \cdot m$) were linked to hydrothermal alteration minerals such as illite, chlorite, and biotite, suggesting thermal gradients and possibly multiple reservoir zones. These results confirm the structural control of the system, with conductive anomalies aligned to the Cali–Patía and Guachucal faults, reinforcing their role as preferential pathways for hydrothermal circulation.

Building on geophysical surveys and geochemical analyses, Alfaro et al. (2015) proposed a preliminary conceptual model of the Azufral geothermal system. This synthesis integrates gravity, magnetics, geoelectrics, and seismic monitoring with hydrothermal alteration and fluid chemistry to delineate the system's architecture. The model identifies a magmatic heat source at ~4 km depth, a high-temperature reservoir (250–280 °C) hosted in fractured lavas and ignimbrites at 2–2.5 km, and a cap seal formed by hydrothermally altered pyroclastics and low-permeability lavas. Upflow zones are structurally controlled by the Cali–Patía, Tercán–Chimangual, and Azufral–Sapuyes faults, while outflow extends eastward along NW–SE structures toward Sapuyes hot springs. Recharge is interpreted as local, via infiltration through faults and permeable deposits. This integrated model (Figure 17) highlights the structurally controlled nature of the system and confirms Azufral as one of Colombia's most promising high-enthalpy geothermal prospects.

Figure 16. Interpretation of the 2D MT models of the Azufral Volcano, by Rodríguez-Rodríguez, 2022.



Sapuyes' Healt source

NW

Rain

Hydrothermal Fumarole of 85 °C

Domes

NAMATER Table

Outflow

Lat's

Healt source

NE

Figure 17. Conceptual model of the Azufral geothermal system showing the magmatic heat source, reservoir, cap seal, recharge zones, and structurally controlled outflow toward Sapuyes hot springs. Taken from Alfaro et al., 2015.

6 Paipa Geothermal Area

The Paipa geothermal area is located in the axial zone of the Eastern Cordillera of Colombia, ~150 km northeast of Bogotá and 5 km south of the city of Paipa. The area lies at 2,500–2,650 m a.s.l. in gently sloping terrain, with easy access and existing infrastructure, which provides favorable logistical conditions for geothermal exploration (Bona and Coviello, 2016).

Thermalism at Paipa has been recognized since the 19th century, with early studies focused on the chemical composition and therapeutic uses of hot springs. More systematic geothermal research began in 2002, when the Colombian Geological Service (then INGEOMINAS, now SGC), in collaboration with the National University of Colombia, incorporated Paipa into its exploration program (Aguilera et al., 2019).

A preliminary conceptual model of the geothermal system was first proposed by Alfaro et al. (2005), based on surface studies of geology, hydrothermal alteration, and geochemistry. Later contributions expanded this framework, including inventories of hot springs, isotopic studies of low-temperature meteoric waters, hydrothermal alteration mapping, and geophysical surveys (geoelectrics, gravimetry, magnetics, and MT). These data supported the definition of an updated conceptual model for Paipa (Aguilera et al., 2019).

Hydrochemistry indicates that Paipa hot springs are mainly saline sulfate waters of low temperature, long recognized for their therapeutic value and currently exploited in spas and tourism. Their chemical and isotopic composition suggests infiltration of meteoric water through normal faults, recharge in permeable sedimentary rims, and heating by residual magmatic intrusions beneath igneous domes (Aguilera et al., 2019).

More recently, Alfaro et al. (2020) presented a new conceptual model integrating geological,

hydrogeochemical, geophysical, and structural data. This updated framework provides the most complete representation of the Paipa geothermal system to date and guides the planning of a deep exploration well.

6.1 Geology

The Paipa geothermal area is located in the axial zone of the Eastern Cordillera, where the basement is composed of Paleozoic sedimentary and metamorphic rocks (phyllites, schists, gneisses), intruded by Jurassic igneous bodies, and interpreted as the subsurface continuation of the Floresta Massif (González-Idárraga, 2020). Overlying this basement is a thick Mesozoic–Cenozoic sedimentary succession including, from base to top, the Tibasosa, Une, Churuvita, Conejo, Plaeners, Los Pinos, Labor–Tierna, Guaduas, Bogotá, and Tilatá formations. These units comprise shales, sandstones, limestones, and conglomerates, many fossiliferous and locally phosphatic or coal-bearing (Alfaro et al., 2010; González-Idárraga, 2020). Quaternary deposits of alluvial and fluvio-lacustrine origin (sand, silt, clay, and conglomerates) cover low-lying áreas. About 31 km² of the 130 km² mapped area are occupied by Neogene volcanic products, including domes and pyroclastics associated with residual magmatic activity (Alfaro et al., 2010).

Structurally, Paipa lies within a compressional regime linked to the Andean orogeny, characterized by tectonic inversion since the Cretaceous. The area shows both thick-skinned tectonics (basement-involving faults such as Lanceros and Soapaga) and thin-skinned deformation (cover-only thrusts such as El Bizcocho and El Batán, verging SE from the Boyacá Fault) (González-Idárraga, 2020). Transverse faults, including Cerro Plateado and Paipa—Iza, represent reactivated extensional structures active during uplift (Alfaro et al., 2010). Recent tectonism is also recorded by the El Hornito and Cánocas faults, which offset the sedimentary sequence laterally and locally interact with longitudinal faults to create zones of enhanced fracturing (Alfaro et al., 2010). These structural and lithological conditions are critical for the geothermal system. Fractured sandstones, interbedded shales, and intrusive contacts act as hydrogeological reservoirs, while transverse and longitudinal faults provide permeable pathways that favor fluid circulation, hydrothermal alteration, and residual magmatism (Alfaro et al., 2020; SGC, 2016).

Later, the Colombian Geological Survey (SGC), described Paipa as a geothermal system controlled by Neogene domes intruded into a thick Mesozoic–Cenozoic sedimentary sequence and by a network of reactivated faults. Unlike volcanic-driven systems such as Nevado del Ruiz or Azufral, Paipa is interpreted as a non-volcanic geothermal system, where residual magmatic heat and tectonic reactivation drive hydrothermal circulation. Structural control by the Paipa–Iza fault and associated transverse faults (El Hornito, Cánocas) has been identified as the main factor governing fluid upflow and surface thermal manifestations (Alfaro et al., 2020) (Figure 18).

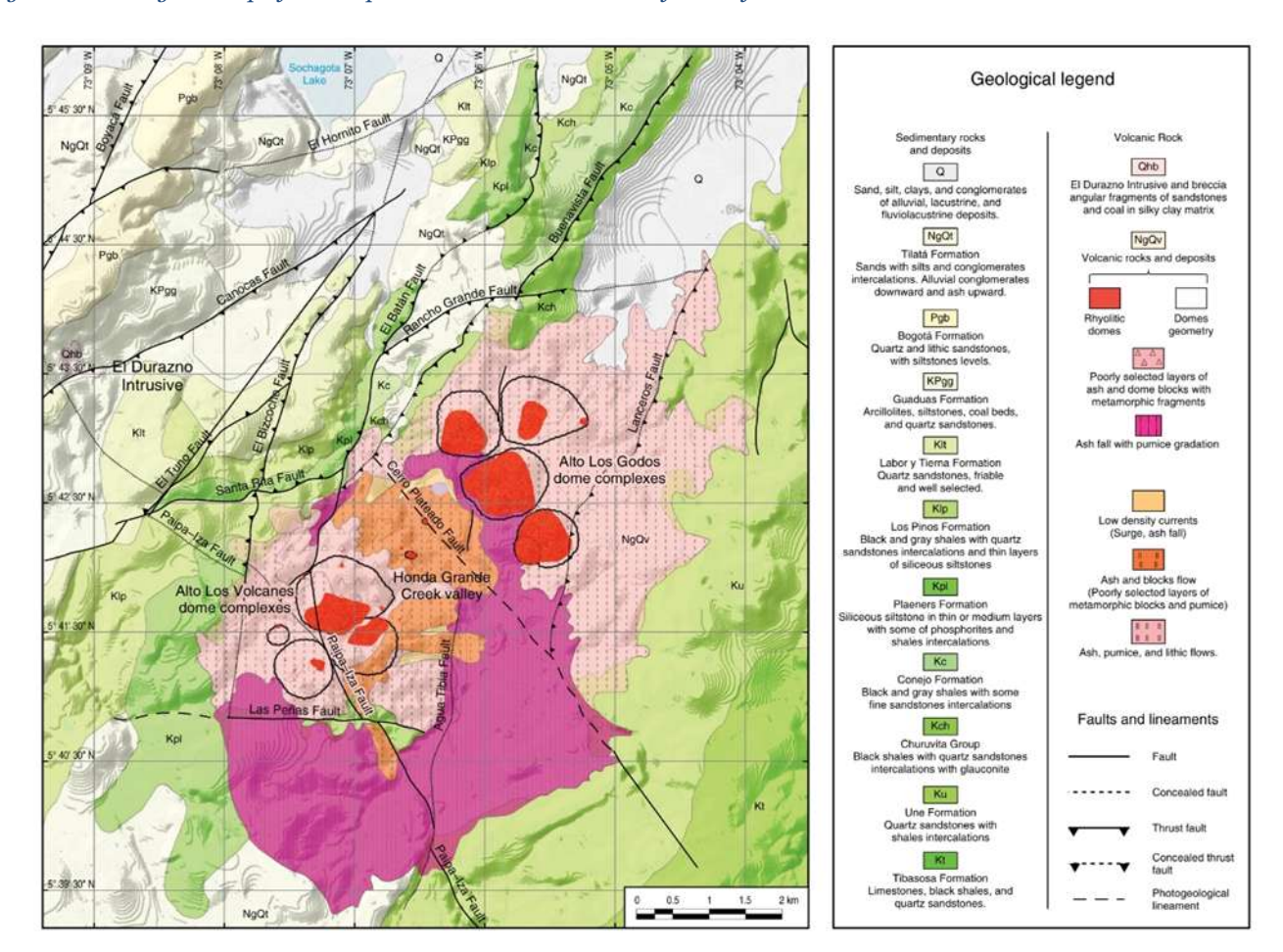


Figure 18. Geological map of the Paipa Geothermal Area. Taken from Alfaro et al. 2020.

6.2 Geochemistry

The first geochemical characterizations of Paipa thermal waters (Ferreira & Hernández, 1988) described a system heated by magmatic intrusions, with a reservoir >200 °C hosted in the Une Formation, sealed by clay-rich Churuvita strata, and recharged through Une outcrops and NE–SW faults.

Later analyses by Alfaro (2002) quantified major and minor species (Na, K, Ca, Mg, Cl, SO₄, HCO₃, Li, Sr, B, F, SiO₂), highlighting extremely high salinities (up to 55,800 mg/L TDS). This salinity "masks" the geothermal signal, producing waters mostly classified as sulfate. Spatial trends indicated a saline focus to the NE, while maximum SiO₂ concentrations (98 mg/L) were recorded at Piscina Olitas in the south, and maximum F values in La Playa and ITP springs, where the hottest discharges occur. The Iza springs, hot but low in salinity, likely represent diluted geothermal reservoir waters (Alfaro et al., 2020) (Figure 19).

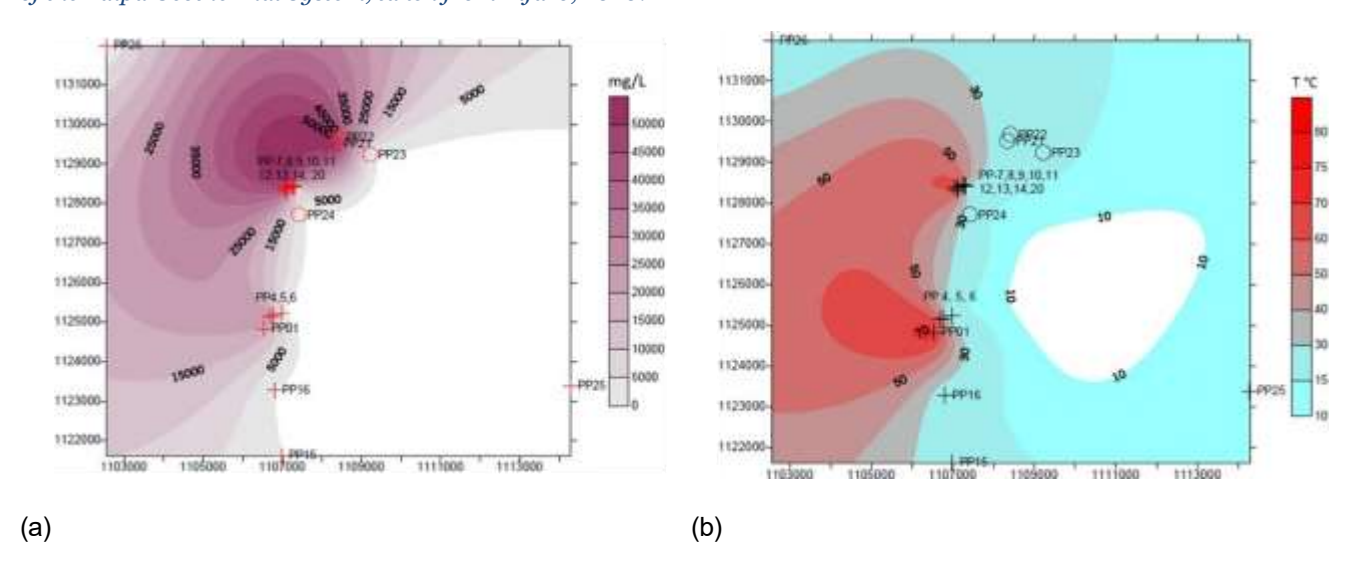


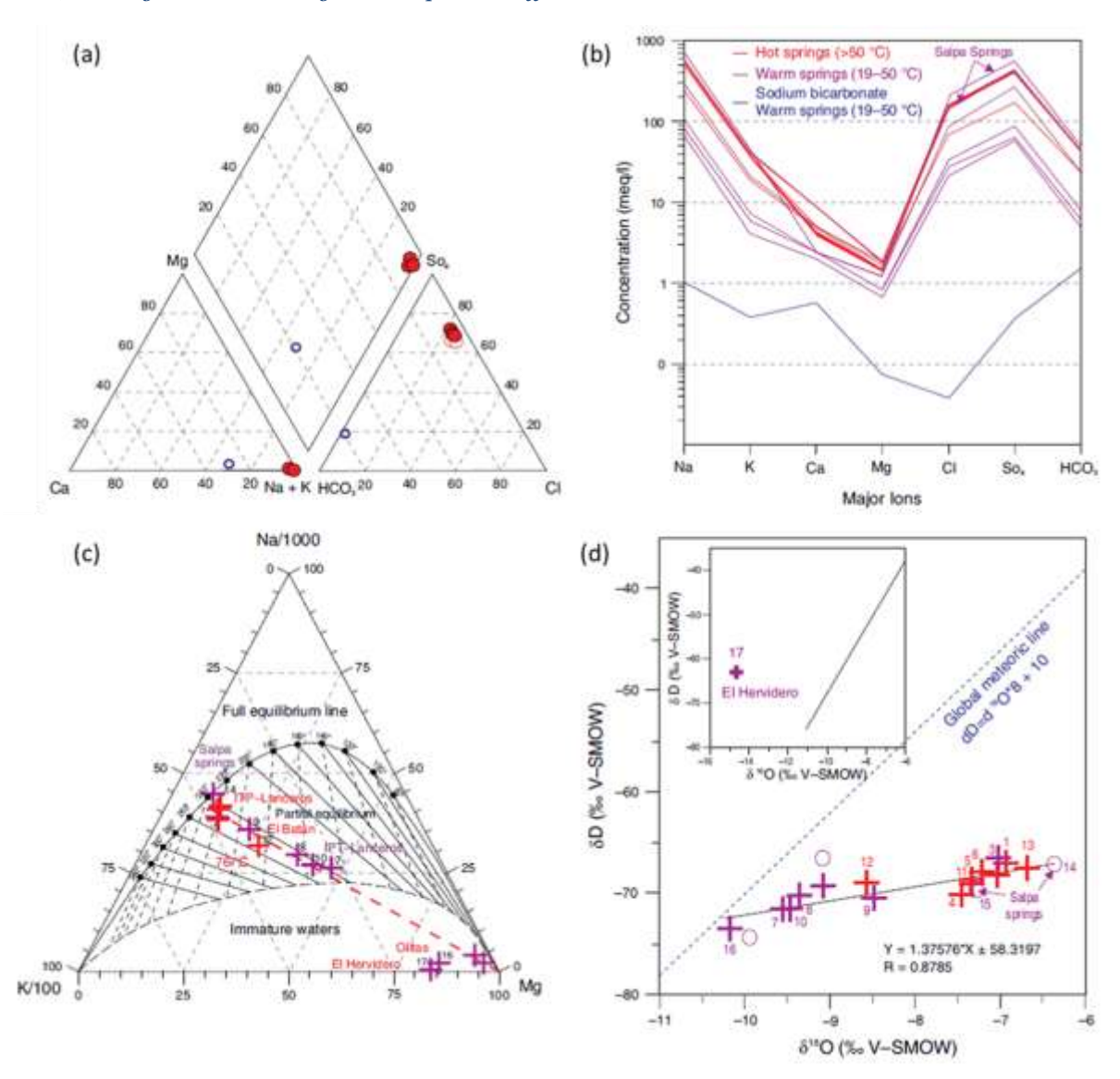
Figure 19. (a) Total dissolved solids (mg/L), in Paipa springs. (b) Contour map showing surface temperatures of the springs of the Paipa Geothermal System, taken from Alfaro, 2020.

More recent syntheses reaffirm that Paipa fluids classify as hyperthermal, strongly mineralized waters, mostly alkaline, but with local acidic springs (Gómez, 2019). Stable isotope data confirm significant evaporation and vapor separation effects. The chemical and isotopic characterization of Paipa hot springs is summarized in Figure 20. Classification diagrams confirm the dominance of strongly mineralized sulfate waters, while Schoeller plots highlight the anomalously high SO_4 contents of the hottest springs. The Na–K–Mg ternary diagram indicates immature waters lacking full equilibrium with reservoir minerals, consistent with mixing processes. Stable isotopes (δD – $\delta^{18}O$) confirm meteoric recharge with significant evaporation and vapor separation effects (Alfaro et al., 2020).

Geothermometric estimates vary widely. Surface spring temperatures reach 77 °C, suggesting reservoir minima of 100–120 °C (silica geothermometer). Other aqueous geothermometers (Na/K, Na–K–Ca, K/Mg) yielded values up to 250 °C, but are unreliable due to disequilibrium conditions (Alfaro, 2002). Isotope-based geothermometry indicates 220–230 °C (Bertrami et al., 1992).

Gas geochemistry adds complexity. Alfaro et al. (2010) reported non-equilibrium compositions in six springs, with estimated temperatures ranging 220–335 °C depending on geothermometer (CO–CO₂–CH₄, CO₂/Ar, ¹³C exchange). Results suggested mixing with a non-geothermal saline source and with gases of organic origin from hydrocarbon-bearing strata.

Figure 20. Hydrochemical characterization of the Paipa geothermal system (Alfaro et al., 2020). (a) Piper diagram; (b) Schoeller diagram of major ions; (c) Na–K–Mg ternary diagram indicating immature waters; (d) stable isotope composition (δD vs $\delta^{18}O$), showing meteoric recharge and evaporation effects.



6.3 Hydrothermal Alterations

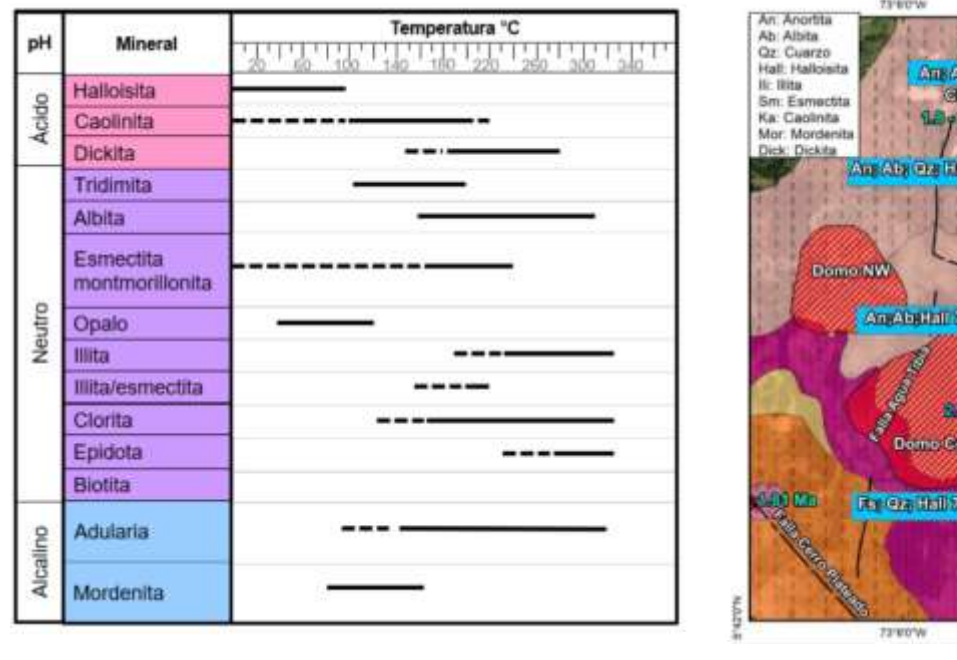
Surface hydrothermal alteration in the Paipa geothermal area (AGP) results from interaction between low-temperature acidic fluids and volcanic–sedimentary deposits. Dominant mineral assemblages include sanidine, quartz, kaolinite, and alunite, with acid alteration extending to depths of 50–100 m (Alfaro et al., 2020).

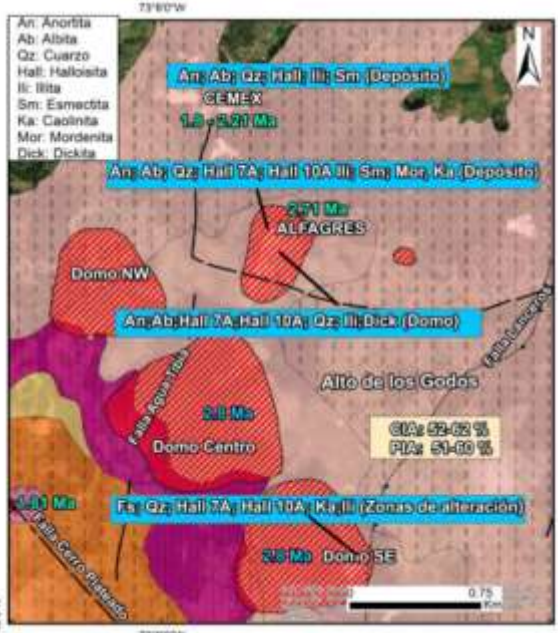
Characterization of volcanic lithologies and hydrothermal overprints in the Alto de los Godos, CEMEX quarry, and ALFAGRES sectors highlights widespread argillic alteration in pyroclastic deposits, evidenced by kaolinite and the smectite–illite series, consistent with formation at 100–200 °C (García Lara, 2021). In contrast, the ALFAGRES sector and the southeastern dome of Alto de los Godos show 7Å and 10Å halloysite, indicating neutral pH and lower-temperature alteration (70–100 °C). X-ray diffraction of volcanic deposits reveals oxidation overprinting, with kaolinite coatings on pyroclastics and

hematite-limonite stains (Alfaro et al., 2020) (Figure 21).

High-temperature alteration is preserved in xenoliths from the upper Los Volcanes sector. Sedimentary and rhyolitic clasts exhibit plagioclase replacement by epidote and chlorite—albite vein infillings, suggesting alteration above 220 °C. Metamorphic xenoliths record even higher conditions, with veins of biotite, adularia, and quartz indicating alteration up to 320 °C (Alfaro et al., 2020).

Figure 21. (a) Hydrothermal alteration minerals in the Paipa Geothermal Area. (b) Distribution map of alteration minerals in domes and deposits of the Alto de los Godos sector of the Paipa Geothermal Area. Modified from García Lara, 2021.





(a) (b)

6.4 Geophysical Studies

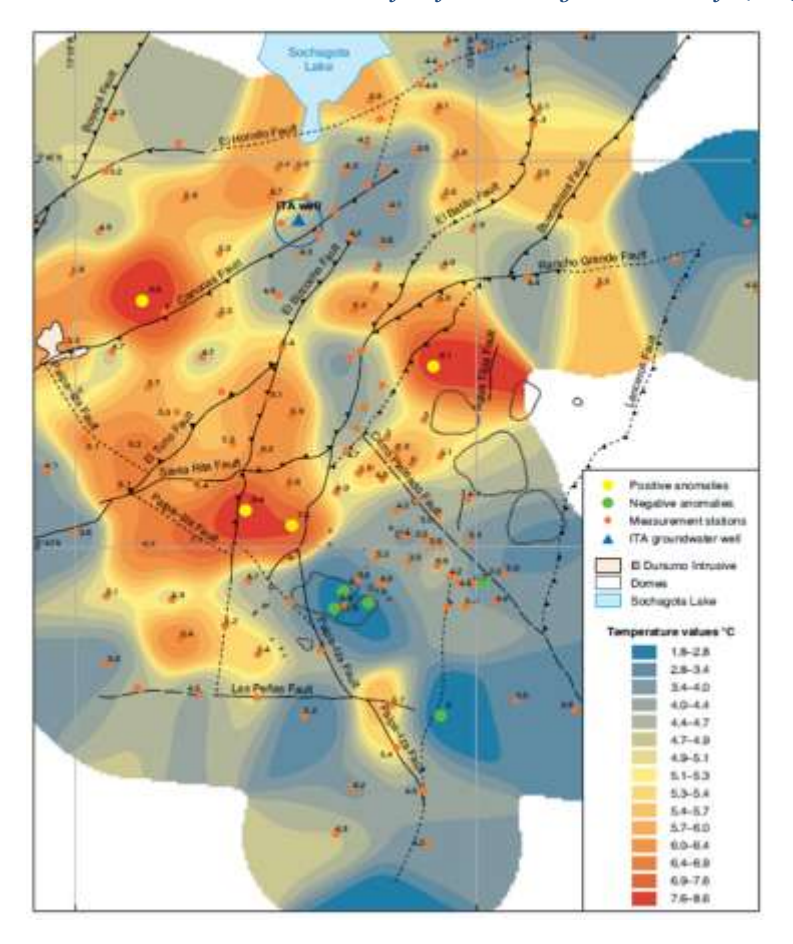
Geophysical studies in the Paipa geothermal area have employed a wide suite of methods to resolve the structural and thermal architecture of the system. Vertical electrical soundings identified resistivity contrasts to ~160 m depth, sensitive to Quaternary deposits and groundwater saturation, while magnetometry revealed spatial variations in magnetic anomalies that correlate with fault traces at depth (Gómez, 2019). These results indicate that the main discharge zones of the geothermal system are structurally controlled, particularly at the junction of the El Bizcocho and El Hornito faults, where fault intersections act as preferential pathways for hydrothermal upflow.

Complementary surveys conducted by Alfaro et al. (2017) included soil temperature profiles (141 stations at 1.5 m depth), which revealed positive thermal anomalies near the intersection of the El Bizcocho, Santa Rita, El Tuno, and Paipa–Iza faults, and around the El Durazno intrusion. Similar results were already recognized in the thermal anomaly map of Rodríguez and Vallejo (2013), which shows clusters of positive surface anomalies aligned with fault intersections, especially near Santa Rita and El Durazno (Figure 22). These observations confirm the structural control of shallow thermal manifestations and highlight the importance of fault junctions in channeling geothermal fluids.

Gravimetric data defined three key features: (1) a large positive anomaly attributed to the Tibasosa–Toledo metamorphic basement, (2) igneous intrusions in the Alto Los Volcanes dome sector, and (3) fault-related contrasts, such as the Cerro Plateado Fault. Magnetometry similarly highlighted

anomalies linked to intrusions lacking surface expression, while geoelectric characterization identified zones of high conductivity (1–10 Ω m) consistent with saline groundwater or hydrothermal fluids, especially near the Chicamocha River depression. Together, these findings point to a heterogeneous system where permeability and fluid pathways are strongly fault-dependent.

Figure 22. Surface temperature anomaly map of the Paipa geothermal area, showing positive anomalies concentrated near fault intersections and the El Durazno intrusive dome. Modified from Rodríguez and Vallejo (2013).



Rodríguez and Vallejo (2013) provided gravimetric and magnetic maps that highlight the structural control of the Paipa geothermal system (Figure 23). The Cerro Plateado Fault is associated with a clear gravimetric anomaly but shows no significant magnetic expression, suggesting that density contrasts in the basement are not accompanied by magnetic contrasts, likely due to the predominance of low susceptibility lithologies or hydrothermal demagnetization. These results support the role of the Cerro Plateado and associated structures in channeling hydrothermal fluids, later refined by subsequent density modeling (Alfaro et al., 2020).

Alfaro (2020) presented a 3D resistivity model that integrates the sedimentary cover, the metamorphic basement, and intrusive bodies (Figure 24). The results reveal a conductive sedimentary layer (0–3 Ω ·m) attributed to saline fluid circulation, intermediate resistivities (10–80 Ω ·m) in the basement, and highly resistive domains (500–1000 Ω ·m) corresponding to intrusive rocks such as El Durazno and Alto Los Volcanes domes. This volumetric view consolidates previous geophysical evidence, confirming the structural and lithological controls of the Paipa geothermal system.

Figure 23. Gravimetric (a) and magnetic (b) anomaly maps of the Paipa geothermal area, highlighting structural controls such as the Cerro Plateado Fault. Taken from Rodríguez and Vallejo (2013).

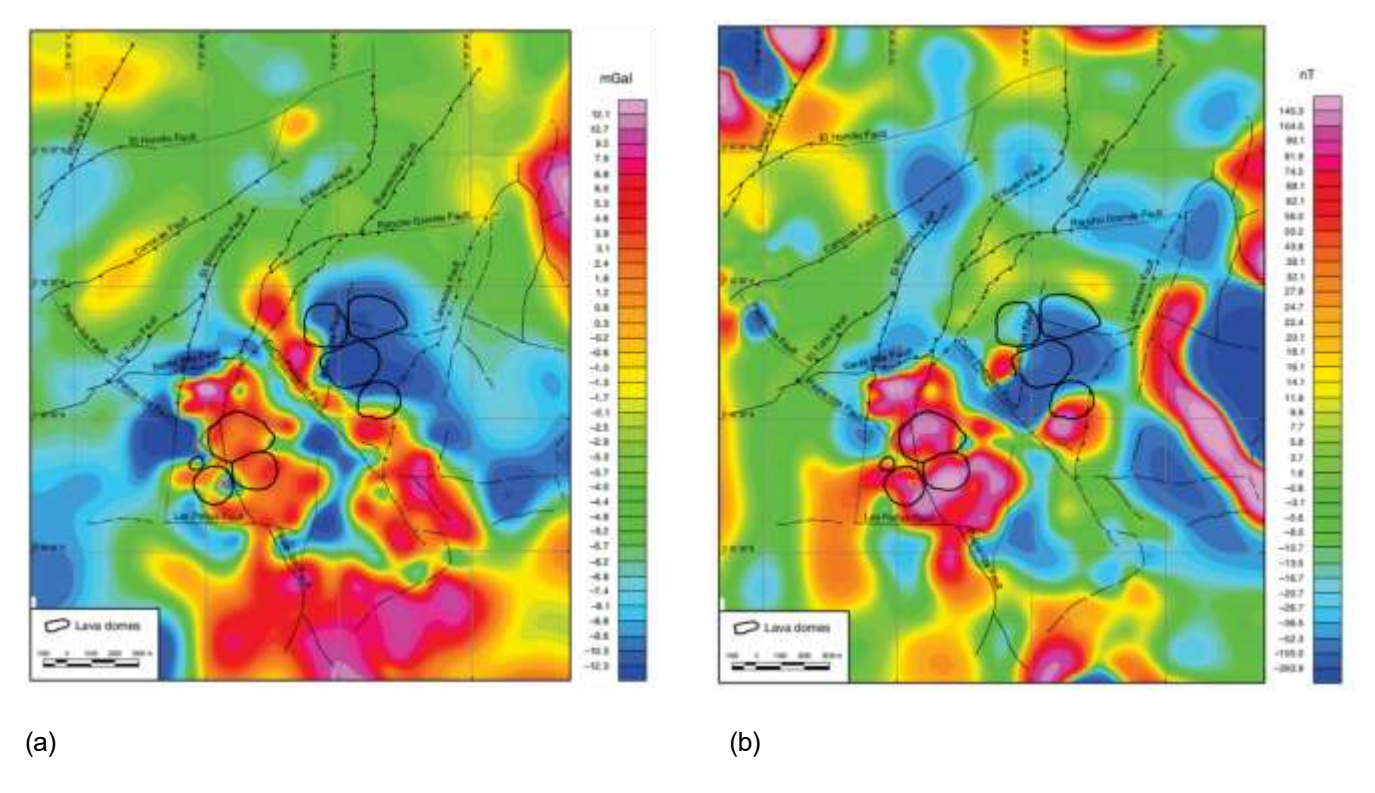
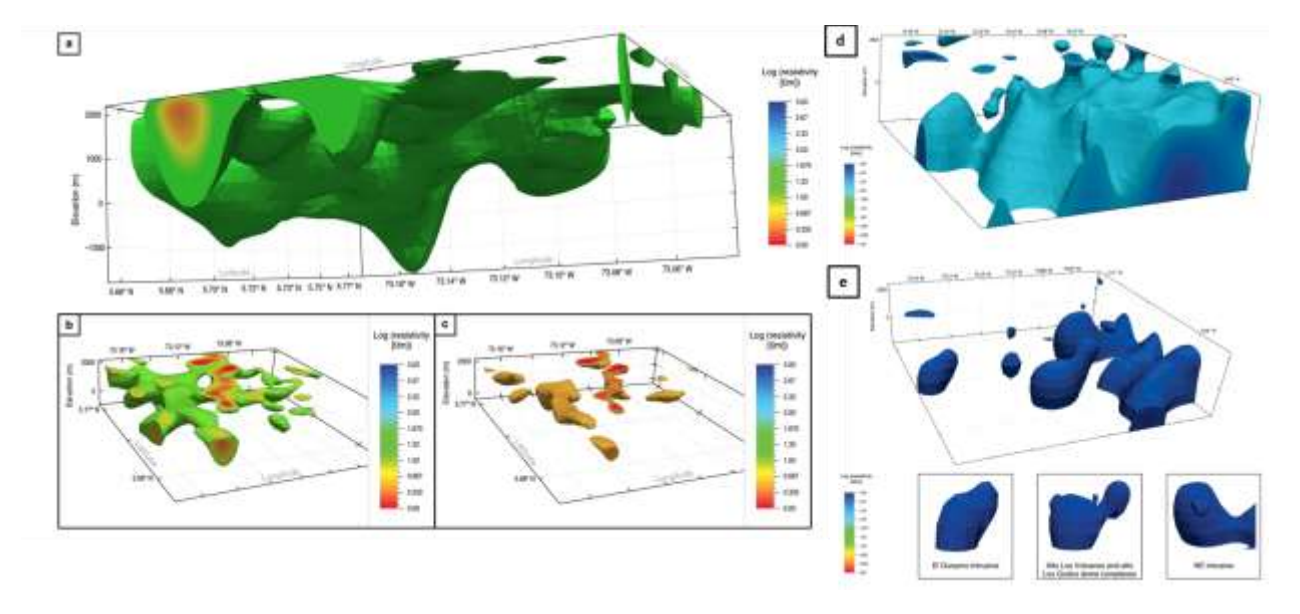
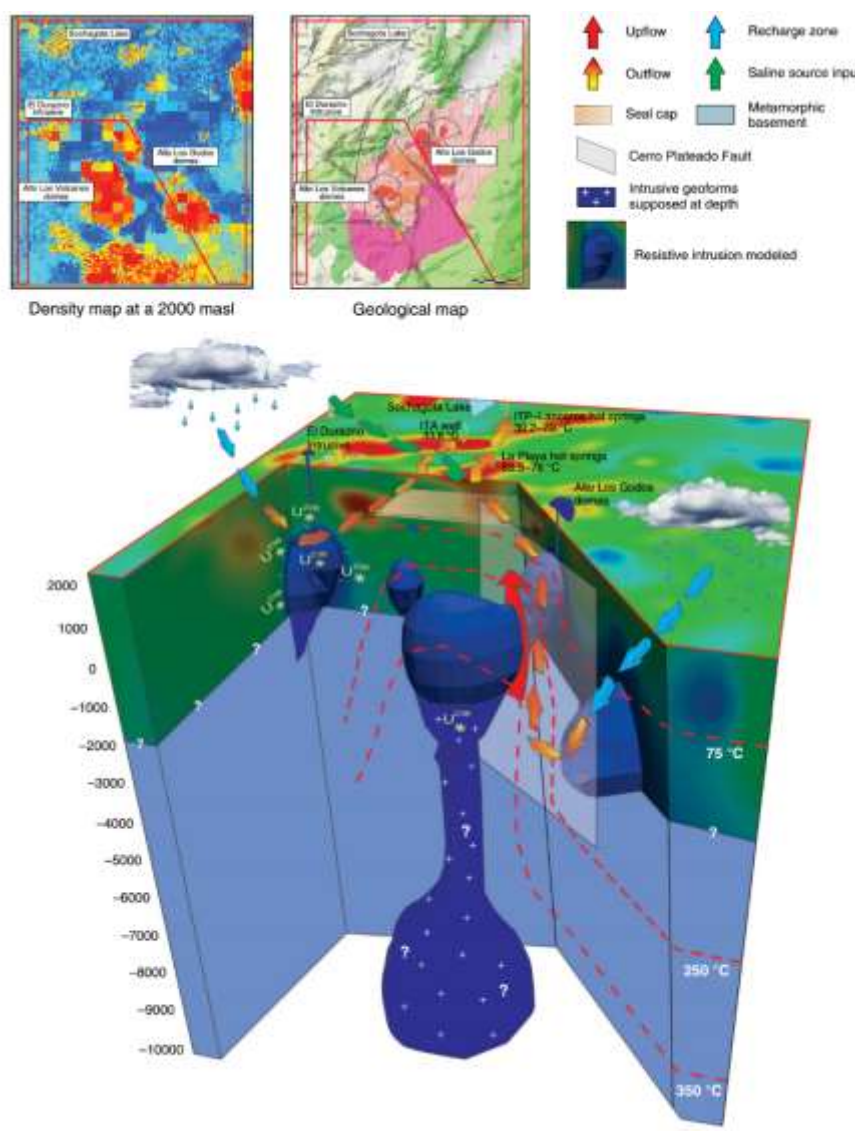


Figure 24. 3D resistivity model of the Paipa geothermal area, highlighting conductive sedimentary layers (a, b, c), intermediate-resistivity basement (d), and resistive intrusive bodies \mathcal{E} . Modified from Alfaro (2020).



Alfaro et al. (2020) showcased a conceptual model for the Paipa geothermal system that integrates geological, geochemical, and geophysical evidence (Figure 25). In this model, fault reactivation within a sedimentary–igneous setting governs hydrothermal circulation, with heat supplied by residual Neogene intrusions and potentially radiogenic sources. Dome-related structures and fault intersections act as preferential fluid pathways. The thermal waters show strong geochemical masking due to mixing with saline aquifers, complicating reservoir characterization but remaining consistent with a magmatic–hydrothermal heat source. This framework defines Paipa as a non-volcanic geothermal system where structural control, rather than recent volcanism, explains fluid circulation and surface manifestations.

Figure 25. Conceptual model of the Paipa geothermal area. The arrows indicate the possible path of water from the recharge areas to the area of interest. Source: Alfaro et al., 2020.



7 Tufiño-Chiles-Cerro Negro Volcanic Complex

The Tufiño - Chiles - Cerro Negro geothermal area is located in the Cordillera Occidental, in the department of Nariño, Colombia and the province of Carchi, Ecuador (on the border of both countries) (Figures 8 and 10). The area of geothermal interest is located around the Chiles (4,730 m.a.s.l) and Cerro Negro (4,470 m.a.s.l) volcanoes. The preliminary geothermal model is based on the general geothermal model consisting of a magma intrusion at a relatively shallow depth (heat source); a formation of permeable rocks that hosts a hot confined aquifer (Reservoir) and a layer of impermeable rocks that form the hydraulic seal and act as a thermal insulator to prevent irradiation of heat accumulated in the reservoir. Gas geothermometers suggest reservoir temperatures of up to 230 °C (Aguilera et al., 2019).

The Chiles - Cerro Negro project is currently in the pre-feasibility stage, and due to its possible temperature, a limit of economic interest was estimated between 15 and 30 MW (Aguilera et al., 2019,

2019), although according to Mejía et al., (2014), the complete system would imply a potential more than 130 MW.

7.1 Geological Setting

The geological evolution of the Chiles–Cerro Negro volcanic area reflects a long history of oceanic crust formation, accretion, magmatism, and tectonic reactivation. Its origin dates back to the Late Cretaceous (Campanian), when the Diabasic and Dagua Groups formed part of the oceanic floor. Oblique accretion of the Caribbean Plate against the South American margin uplifted and eroded the Central Cordillera. Subsequent plate reorganizations, including the fragmentation of the Farallón Plate into the Nazca and Cocos microplates, initiated the Andean orogeny (Bocanegra and Sánchez, 2017).

Magmatic activity has been episodic: Bayona et al. (2012) documented subduction-related volcanism since the Late Cretaceous, a Paleogene Iull, and Miocene reactivation with Nazca Plate subduction. Volcanism resumed in the Upper Pleistocene, producing edifices such as Cagüil, Cerro Crespo-Nasate, and Cerro Colorado, and later the Chiles and Cerro Negro volcanoes. Activity persisted until ~200 ka, with Chiles exhibiting its last effusive activity ~15 ka, and Cerro Negro showing eruptive activity as recently as ~6.2 ka (Bocanegra & Sánchez, 2017).

The structural framework is complex, with chevron-style folding (W-vergent) in Cretaceous units and a dominant N20°E fault trend. Major structures include: the Guachucal Fault (dextral, oblique planes N55°E to N55°W), the Chiles–Cumbal Fault (continuation of the Cauca–Patía Fault, associated with Río Blanco hot springs), the Nasate Fault (NW–SE, affecting the Nasate volcano), the Chiles–Cerro Negro Fault (crosscutting both craters, linked to "Aguas Hediondas" springs in Ecuador), and the Tufiño Fault, which aligns volcanic centers along a N30°E trend (Bocanegra and Sánchez, 2017). Additional transverse faults, such as Chiles-North and Cerro Negro–Nasate, further disrupt the volcanic complex.

Petrostratigraphy reveals parallel volcanic histories. Chiles Volcano underwent six effusive episodes, from early andesitic lavas to dacitic domes and columnar flows, reflecting alternating andesitic and dacitic magmatism (García and Sánchez, 2019). Cerro Negro Volcano, in contrast, records five eruptive episodes, including both blocky dacitic lavas and pyroclastic flows, overlying early andesitic foundations (Cortés and Calvache, 1996). Fallout deposits from Azufral or Ecuadorian volcanoes are also intercalated. Collectively, these volcanic sequences demonstrate the alternation of effusive and explosive phases typical of stratovolcanoes in active arc settings (Figure 26).

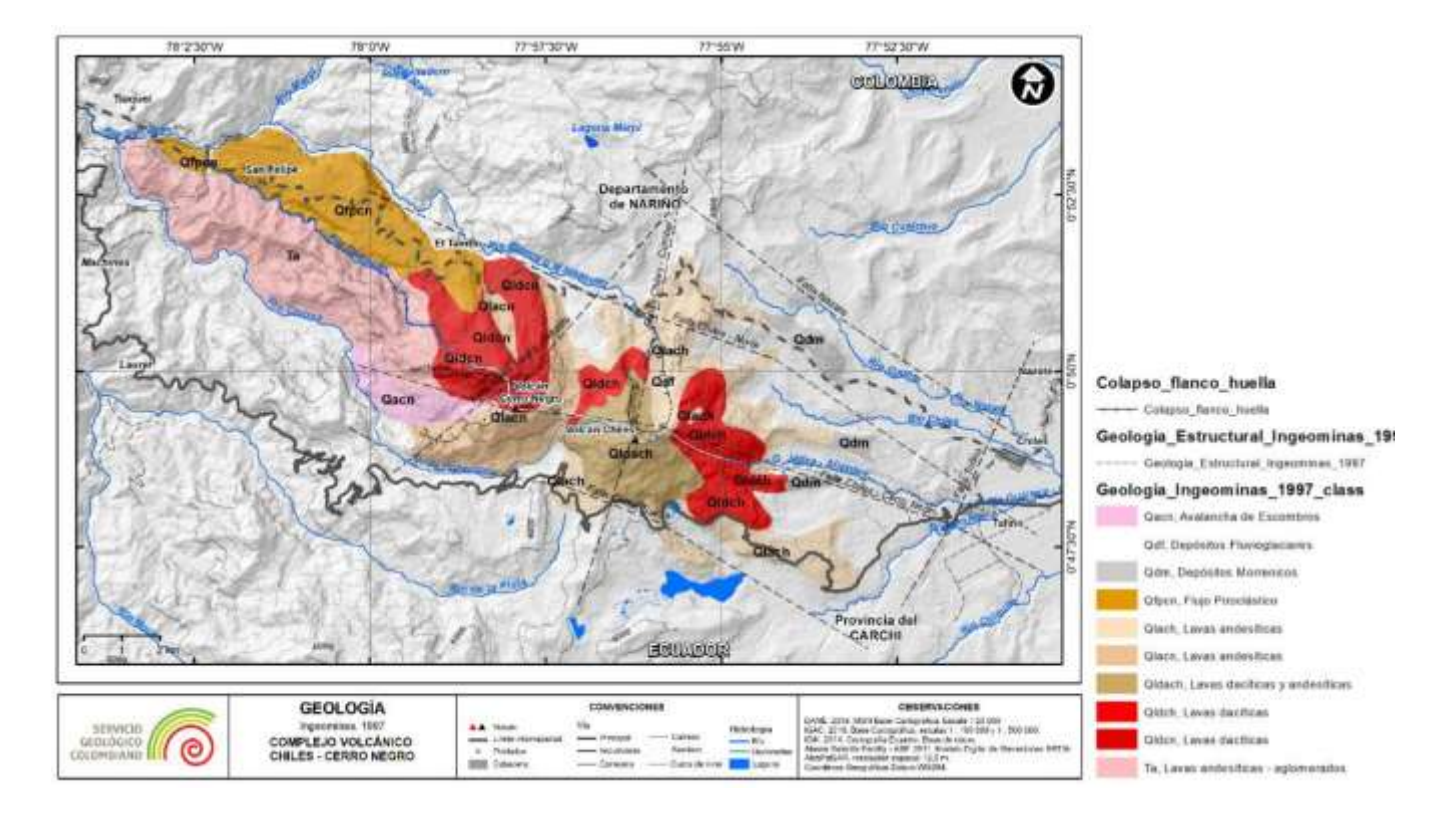


Figure 26. Simplified geologic map of the Chiles - Cerro Negro volcanic complex Taken from Cortés et al., (2023).

7.2 Geochemistry

Hydrogeochemical surveys by ICEL (1983) and OLADE (1987) outlined a stratified geothermal system beneath the Chiles–Cerro Negro complex. Two productive horizons were defined: (i) a shallow aquifer at 500–1000 m depth, with temperatures near 150 °C, and (ii) a deeper reservoir, close to 2000 m depth, exceeding 200 °C and considered the main exploration target. The shallow sequence hosts calcic bicarbonate waters of very low salinity at the surface, while geothermometric anomalies suggest mixing with deeper, hotter fluids. Overlying volcanic deposits altered to clays form an impermeable cap (stratum B), restricting vertical flow except along fractures. Geochemical balances also suggest the existence of an additional aquifer beneath this seal, below 1300 m, with temperatures of industrial relevance (OLADE, 1987). Recharge occurs through infiltration along mountain ridges, with flows directed toward both eastern and western flanks, circulating mainly through Pliocene volcanic sequences (ICEL, 1983).

In the prefeasibility phase, ICEL (1983) analyzed 28 thermal and cold water samples over a 900 km² area, measuring pH, temperature, and major and minor ion concentrations (Na $^+$, K $^+$, Ca $^{2^+}$, Mg $^{2^+}$, HCO $_3$ $^-$, SO $_4$ 2 $^-$, SiO $_2$, Li $^+$, Fe $^{3^+}$, Sr $^{2^+}$). Waters were grouped into distinct chemical facies reflecting rock–fluid interaction at depth (Figure 24). Six representative samples were also subjected to geothermometric evaluation using silica, Na–K, and Na–K–Ca indices (Table 3).

The results indicate three broad behaviors: (i) bicarbonate waters reflecting meteoric dilution and disequilibrium at shallow levels, (ii) bicarbonate waters trending toward equilibrium with feldspathic rocks at depth, and (iii) sulfate waters in marked disequilibrium. Among the applied indices, the Na–K–Ca geothermometer provided the most consistent results, estimating an average reservoir temperature of ~224 °C (Table 4), reinforcing the interpretation of a high-enthalpy system (ICEL, 1983).

Table 3. Temperature estimates in °C at depth for each sample, according to each geothermometer. Source: ICEL, 1983.

Sample No.	Silica Eq. 1	Silica Eq. 2	Sodium-Potassium	Sodium-Potassium-Calcium
MFAH-1	104	102	398	238.5
MFAN-2	122	123	343	233.1
MFAL-3	89	85	320	191
MChC1-4	113	112	386	233.8
MChC2-5	89	85	375	226.1
MChB1-6	120	121	355	219.2

Table 4. Chemical types of waters in the Tufiño-Chiles-Cerro Negro geothermal system. Source: ICEL, 1983.

Chemical type	Sub-group	Salinity (meq/L)	Temperature (°C)	Hydrogeological situation	No. of samples
Bicarbonate	Low salinity	1.4 – 6	14	Shallow circuits	7
Bicarbonate	Medium salinity	12 – 26	20 – 40	Deeper circuits interacting with hot gases rich in CO ₂ or areas with high heat flow	8
Bicarbonate	High salinity	41 – 137	14.2 – 32.4	-	6
Sulfated	Alkaline	21 – 28	16.8 – 22.7	Shallow circuits interacting with volcanic gases rich in H₂S. Leaching of hydrothermalized rocks	4
Sulfated	Alkaline	20 – 37	31 – 51.5	Shallow circuits of bicarbonated waters with addition of H_2SO_4 (oxidation of H_2S)	3

More recently, Taussi et al. (2023) carried out a comprehensive chemical and isotopic survey of thermal waters and fumaroles across the Tufiño–Chiles–Cerro Negro (TCCN) system, refining the understanding of fluid origins and evolution. Their results confirm the coexistence of neutral chloride–sodium waters, acid–sulfate waters, and bicarbonate waters, consistent with earlier classifications, but with improved resolution on mixing processes and magmatic inputs.

Stable isotopes (δ^{18} O, δ^{2} H) demonstrate a dominant meteoric recharge modified by interaction with magmatic gases (Figure 27), while CO₂–He isotopes confirm the contribution of deep magmatic fluids. Geothermometers indicate reservoir temperatures ranging from ~200 to 250 °C (Figure 28), in agreement with previous estimates but highlighting local variability linked to structural controls. Overall, their conceptual model depicts a high–enthalpy geothermal system fueled by a magmatic heat source, structurally channeled along the Chiles–Cumbal and Chiles–Cerro Negro fault systems, where water–rock interaction and gas input produce the observed geochemical diversity.

Figure 27. a) and b) δD -H2O versus $\delta^{18}O$ -H2O for TCCN water samples showing the Global and Local Meteoric Water Lines. c) Altitude versus δD isotopic composition of TCCN waters, including the theoretical vertical isotope gradient for Ecuador and comparative data from nearby volcanic and geothermal systems. Taken from Taussi et al. (2023)

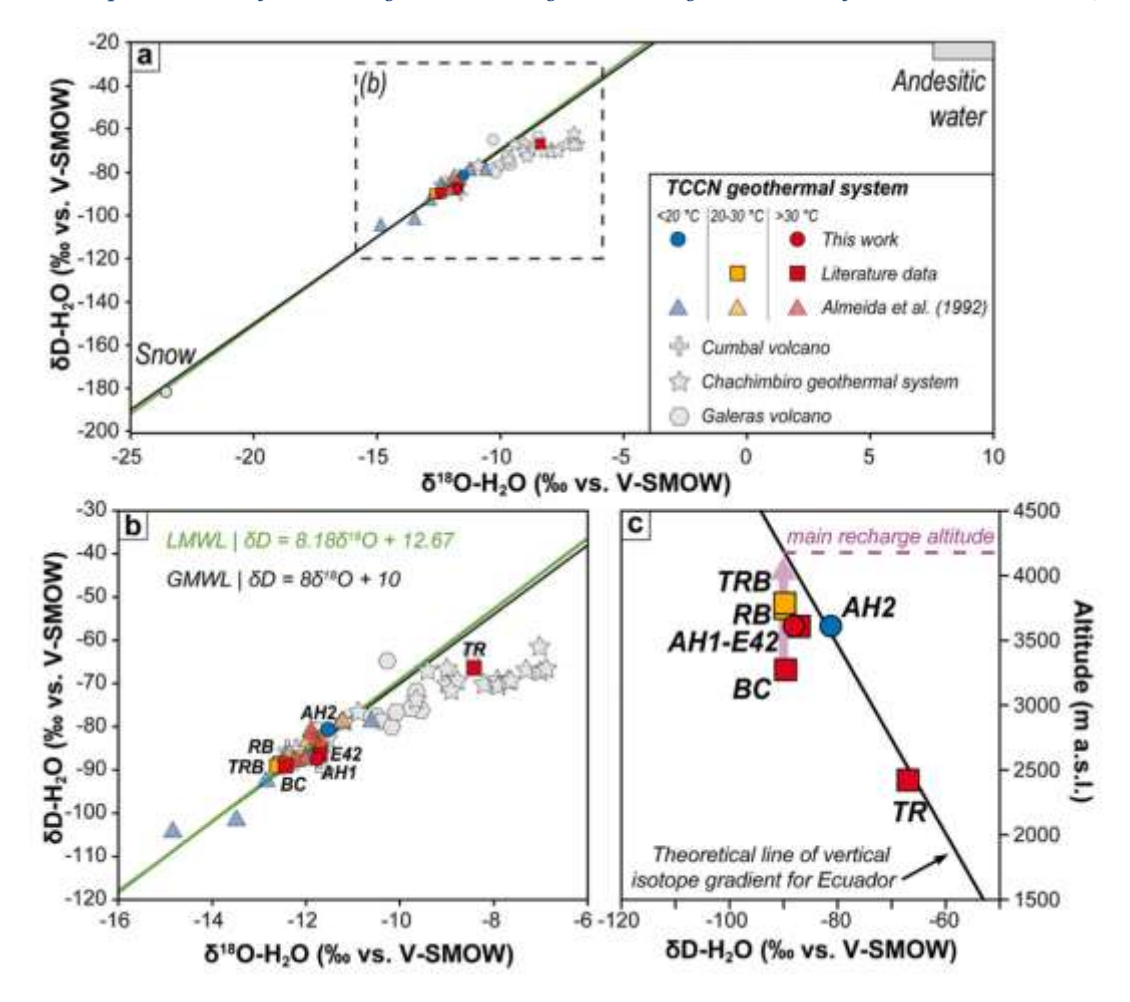
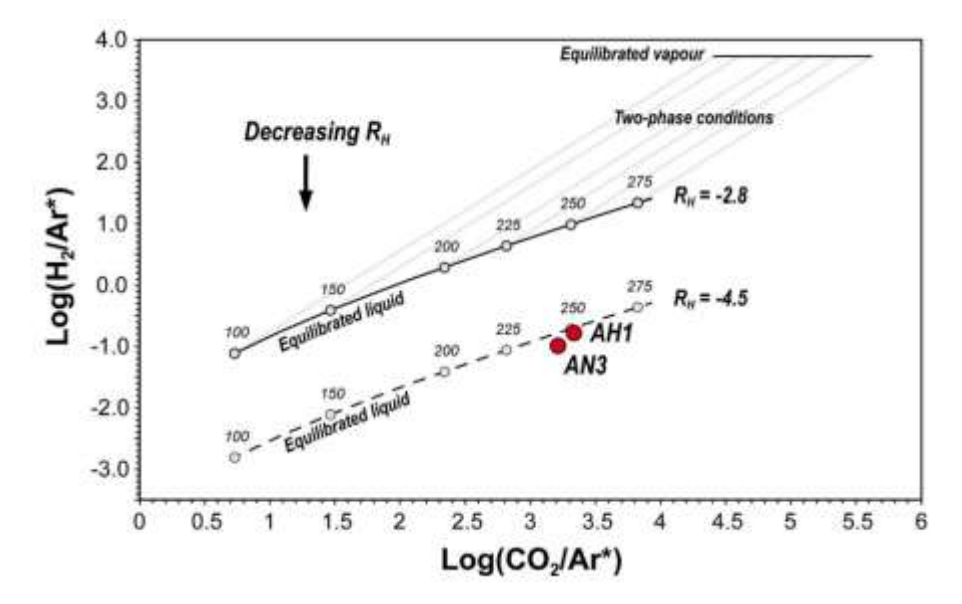


Figure 28. Binary diagram of $Log(H_2/Ar^*)$ versus $Log(CO_2/Ar^*)$. Solid lines indicate equilibria in liquid and vapour phases at temperatures between 100 and 275 °C. The dashed line represents equilibria in a liquid phase under more oxidizing conditions. Taken from Taussi et al. (2023)



7.3 Hydrothermal Alteration

Surface hydrothermal alteration around the Chiles–Cerro Negro volcanic complex is intense and spatially associated with craters, structural intersections, and remnants of collapse structures. Within the craters of Chiles, Cerro Negro, and the glacially eroded Nasate, alteration is particularly marked, while to the north it extends toward the Cumbal domain. Fault intersections near both edifices consistently coincide with fumarolic activity and amorphous silica deposition, delineating the surface boundaries of the geothermal field (ICEL, 1983).

Acid sulfate alteration dominates the higher elevations on both the Colombian and Ecuadorian flanks, especially along road cuts on the northern slopes of Chiles volcano and in the Maldonado corridor. In Ecuadorian territory, thermal springs such as Aguas Hediondas and Aguas Negras display conspicuous silica deposition. Fumarolic alteration and acid-sulfate vapor interaction have produced assemblages of montmorillonite, kaolinite-group clays, opal, and locally alunite. These minerals progressively clog fluid pathways, leading to self-sealing and reduced permeability—a hallmark of argillic alteration zones (ICEL, 1983).

Regional geophysical surveys also point to deep-seated alteration. OLADE (1987) reported a thick conductive stratum beneath the Aguas Hediondas sector and the central–northern portion of the Tufiño depression, interpreted as the product of pervasive hydrothermal alteration of host rocks due to sustained hot-fluid circulation.

Geochemical—isotopic analyses performed by Taussi et al. (2023) confirm that these alteration patterns are closely linked to structural controls and persistent magmatic gas input along major faults. Vapor-dominated zones explain the prevalence of acid—sulfate alteration at high elevations, while neutral chloride and bicarbonate waters reflect deeper liquid-dominated domains. This duality accounts for the coexistence of intense sealing near the surface with more permeable hydrothermal conduits at depth, a configuration that defines the geothermal architecture of the Tufiño—Chiles—Cerro Negro system.

7.4 Geophysics

Pre-feasibility studies conducted by Aquater (OLADE, 1987) and later refined by Coviello (2000) provided the first geophysical framework for the Tufiño–Chiles–Cerro Negro system, combining gravimetric, magnetometric, geoelectric, and magnetotelluric methods. The area is located within a zone of persistent volcanic activity, where a regional heat-flow anomaly is overlain by local anomalies related to the feeding systems of Upper Pleistocene volcanism. The compositional evolution of volcanic products supports the hypothesis of a shallow magmatic chamber capable of generating a significant thermal anomaly (ICEL, 1983; Coviello, 2000).

Magnetotelluric soundings revealed conductive bodies at depths of 3–7 km, extending across several square kilometers and reaching thicknesses of up to 2 km. Their resistivities, ranging from 1 to 10 Ω ·m, suggest zones of enhanced permeability saturated with hot saline fluids, or alternatively, intrusions emplaced along fracture networks. At greater depths of 15–20 km, thermal modeling indicates temperatures of 700–750 °C and geothermal gradients of 36–50 °C/km, values approximately 1.2 to 1.7 times higher than the global average. Surface manifestations are consistent with these anomalies: thermal springs in the Tufiño and Aguas Hediondas sectors discharge at 26–53 °C, considerably above the mean annual air temperature of 9 °C. Geothermometric evaluations indicate equilibrium reservoir temperatures above 100 °C and reaching up to 220 °C in the vicinity of Chiles volcano.

The integrated interpretation of geoelectric, magnetic, and gravimetric data defines a layered stratigraphy composed of three principal units (Table 5). The superficial Layer A shows medium to high resistivities between 100 and 1000 Ω ·m, densities of 2.4–2.6 g/cm³, and elevated magnetic

susceptibility. Within this layer, three electrostratigraphic sublevels can be distinguished: a thin resistive cover only a few tens of meters thick, an intermediate conductive horizon of 50-300 m with resistivities between 10 and $50~\Omega\cdot m$, and a basal resistive level exceeding $500~\Omega\cdot m$. The overall thickness of Layer A can reach up to 1 km, and it hosts both shallow meteoric aquifers and deeper circulation pathways. Beneath this, the Layer B is strongly conductive, with resistivities of $1-30~\Omega\cdot m$, densities of 2.2-2.4 g/cm³, and negligible magnetic susceptibility. This layer, with a thickness between 1 and 2 km but thinning westward to less than 500~m, corresponds to hydrothermally altered volcanic deposits that act as a regional cap rock, though fractures locally permit upward fluid migration. At greater depth, the Layer C exhibits high resistivities of $500-1000~\Omega\cdot m$, densities near 2.7~g/cm³, and strong magnetic susceptibility. It is interpreted as a fractured volcanic or intrusive basement, where permeability is sufficient to allow the circulation of hot saline fluids despite its otherwise resistive character.

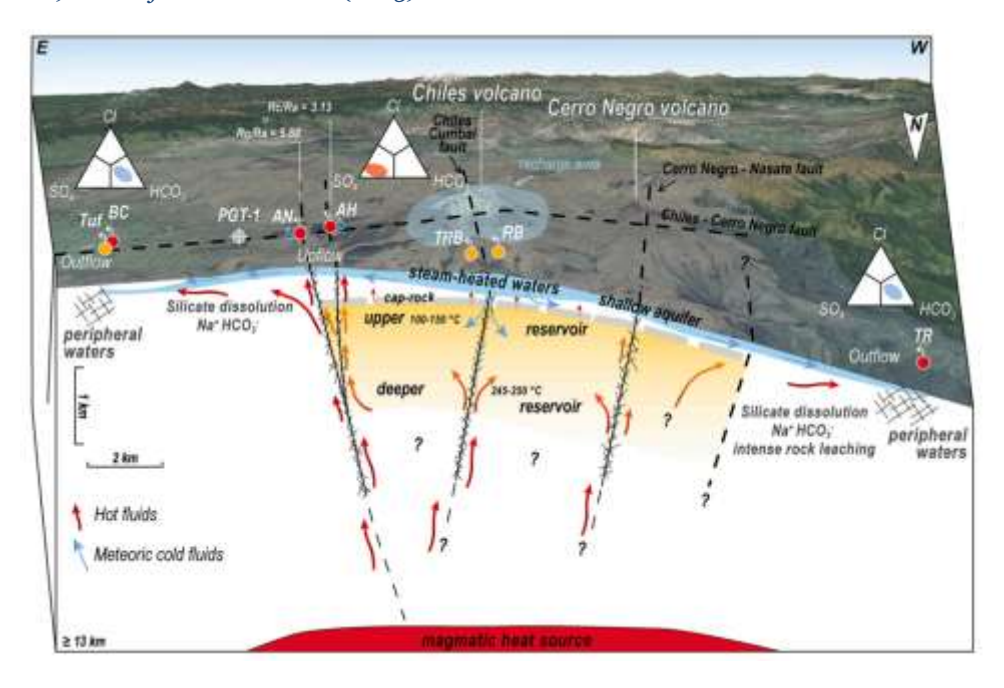
Table 5. Four-electro-layer model of the Tufiño-Chiles-Cerro Negro geothermal system. Taken from Coviello, 2000.

Layer	Thickness	Resistivity
Layer A	Fixed: 800 m	100 Ohm-m
Layer B	Variable	5 Ohm-m
Layer C1	Variable	100 Ohm-m
Layer C2	Infinite	1,000 Ohm-m

This geophysical framework converges on a model in which the geothermal reservoir is hosted within a fractured basement overlain by a thick conductive, hydrothermally altered volcanic sequence acting as a seal. The system is fueled by a regional magmatic heat source, modulated by fault-controlled permeability and localized anomalies associated with the Chiles and Cerro Negro volcanoes.

A conceptual model was proposed by Taussi et al. (2023), integrating geochemical, geological, and geophysical evidence to refine the understanding of the Tufiño–Chiles–Cerro Negro system (Figure 29). Their synthesis identifies a magmatic heat source at ~13 km depth, sustaining a stratified hydrothermal system with at least two reservoirs: a shallow aquifer at 500–1000 m and a deeper reservoir exceeding 1500 m, both capped by a low-permeability altered volcanic sequence. Meteoric recharge above 4100 m mixes with ascending magmatic fluids, producing the observed spectrum of sulfate, bicarbonate, and chloride waters, while gas geothermometry at Aguas Hediondas and Aguas Negras indicates reservoir temperatures of ~245–250 °C. The model highlights the dual role of structural permeability and magmatic degassing in controlling fluid pathways and chemical evolution, supporting the classification of TCCN as a structurally controlled, high-enthalpy geothermal system.

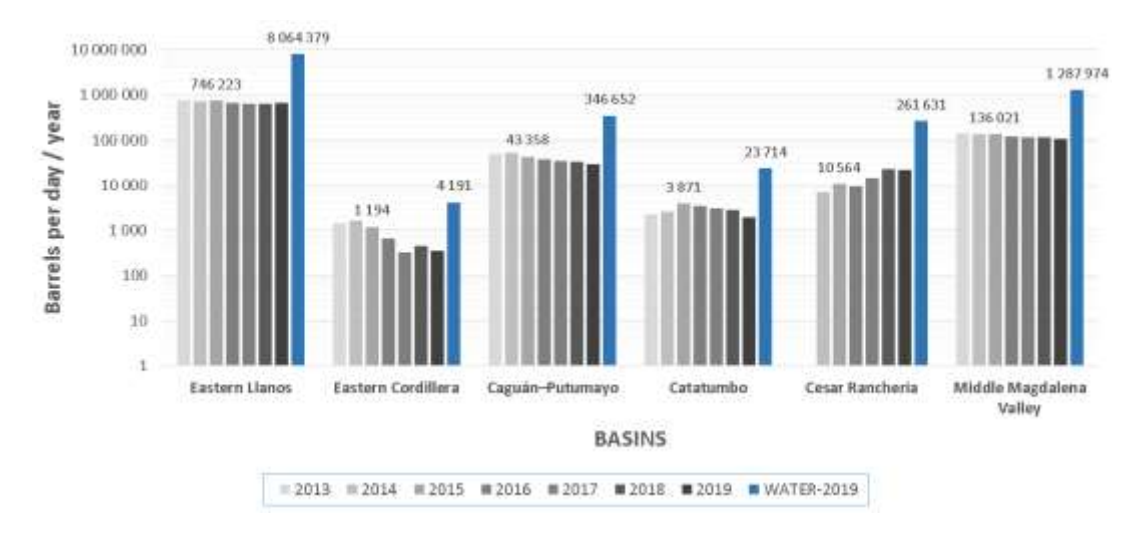
Figure 29. Conceptual model of the Tufino-Chiles-Cerro ~ Negro geothermal system in a schematic E-W oriented cross-section (view from the North). Taken from Taussi et al. (2023).



8 Conduction-dominated geothermal systems

Conduction-dominated geothermal resources in Colombia are mainly associated with sedimentary basins, where the geothermal gradient and oilfield co-produced waters define the potential for electricity generation. National assessments indicate that oil and gas operations currently produce 10–12 million barrels of water per day with temperatures between 42 and 179 °C (Pinto et al., 2021). Using the MIT methodology, this resource represents about 170-287 MWe of technical potential, with individual binary ORC plants capable of generating 200–320 kWe from waters at 80–90 °C. Financial evaluations suggest that such projects can be economically viable, with payback periods of 7–9 years under current Colombian regulations (Pinto et al., 2021) (Figure 30).

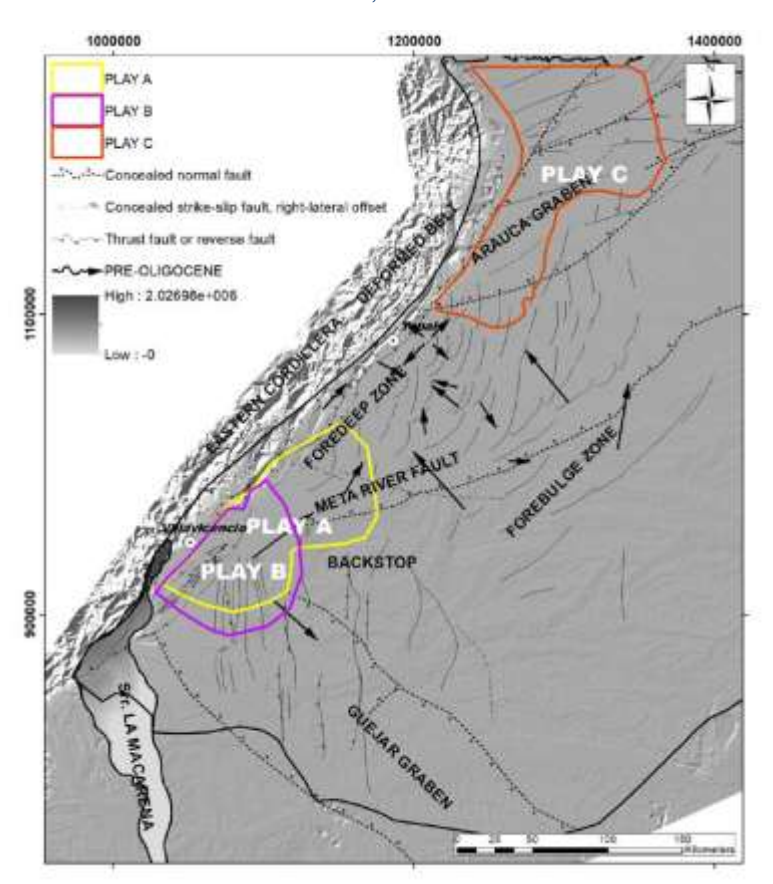
Figure 30. Oil and water co-production in Colombia up to 2019, illustrating the potential of co-produced waters for geothermal use in sedimentary basins (taken from Pinto et al., 2021).



8.1 Eastern Llanos Sedimentary Basin

Among Colombian sedimentary basins, the Eastern Llanos Basin stands out, concentrating more than 80% of the conduction-dominated geothermal potential (Pinto et al., 2021). Recent assessments in this basin have integrated geothermal gradients, reservoir properties, and hydrogeological conditions to outline three regional plays (López-Ramos et al., 2022) (Figure 31): The first involves fractured crystalline basement and Paleozoic rocks, regarded as speculative due to limited drilling data. The second corresponds to the Une Formation sandstones, which behave as semi-confined aquifers recharged from the Serranía de la Macarena; this play has already been tested in producing fields and is considered emergent. The third play also involves Une Formation but under confined conditions at greater depths, where temperatures exceed 100 °C and a pilot ORC plant has demonstrated generation capacity.

Figure 31. Structural map of the Llanos Basin showing the three proposed geothermal plays. Taken from López-Ramos et al., 2022.



Thermal modeling shows that the 100 °C and 200 °C isotherms occur at depths of 2–3 km and 5–6 km, respectively, delineating the most favorable areas for development (Figure 32). A reservoir condition map further highlights sectors with optimal geothermal prospectivity (Figure 33). Complementary conceptual models emphasize the critical role of the Serranía de la Macarena as a recharge zone, where strong hydraulic heads drive regional flow and influence both geothermal circulation and the distribution of heavy oils in the basin (Figure 4).

Figure 32. Depth map of the 100 (a) and 200 (b) °C isotherms in the Llanos Basin, derived from geothermal gradient models (modified from López-Ramos et al., 2022).

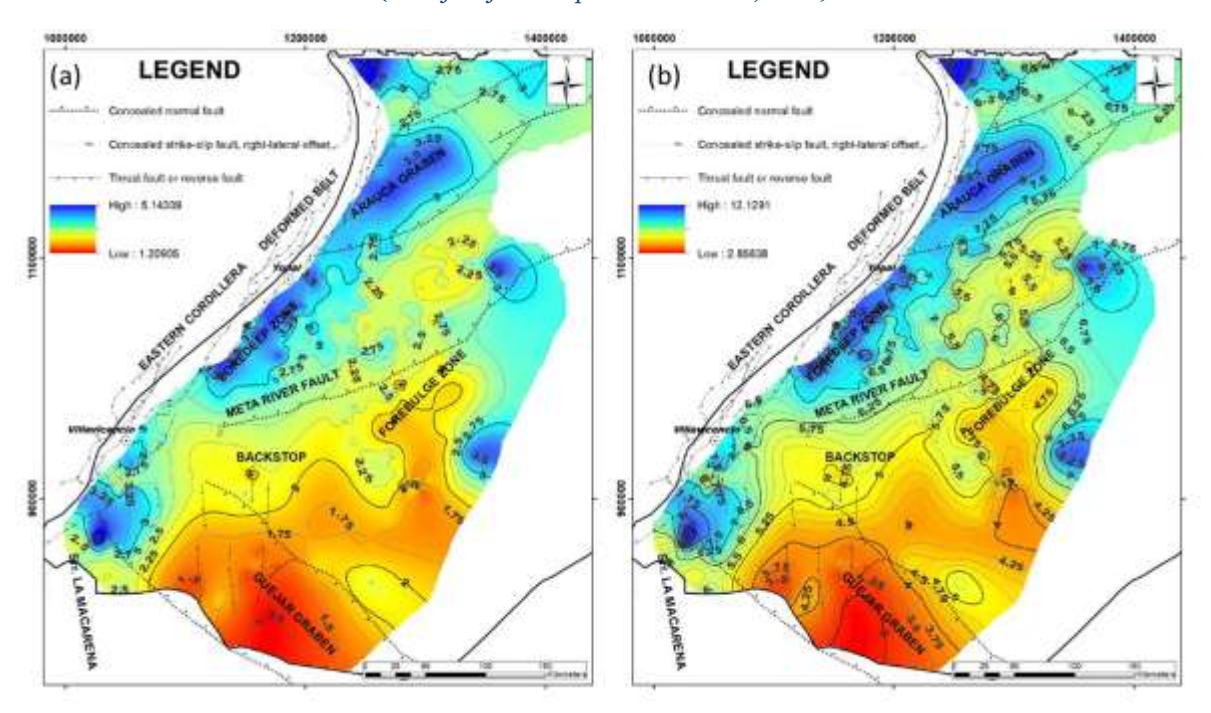
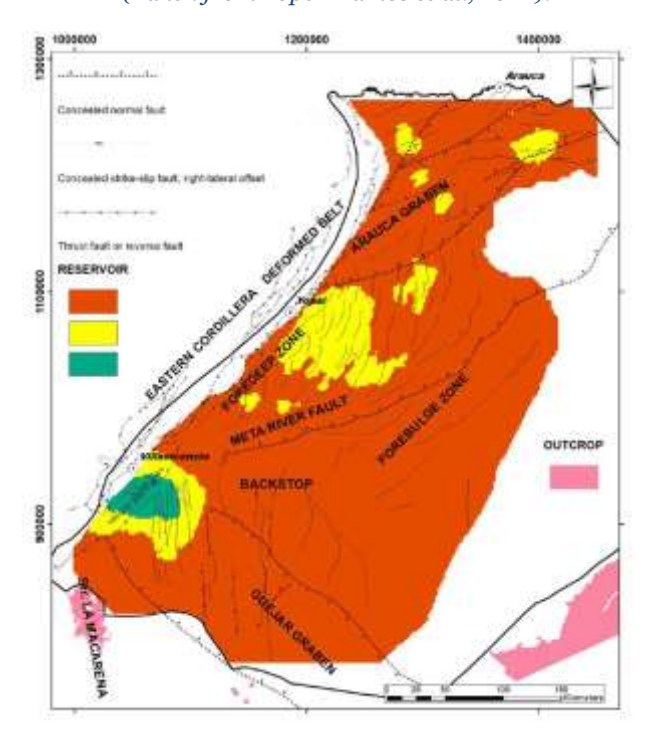


Figure 33. Reservoir condition map of the Llanos Basin, indicating geothermal prospectivity (green = optimal; red = low), (Taken from López-Ramos et al., 2022).



Altogether, these results position the Llanos Basin as the country's most promising conduction-dominated geothermal province, providing a strategic counterpart to the high-enthalpy volcanic systems of the Andes and illustrating the role of co-produced waters in Colombia's energy transition.

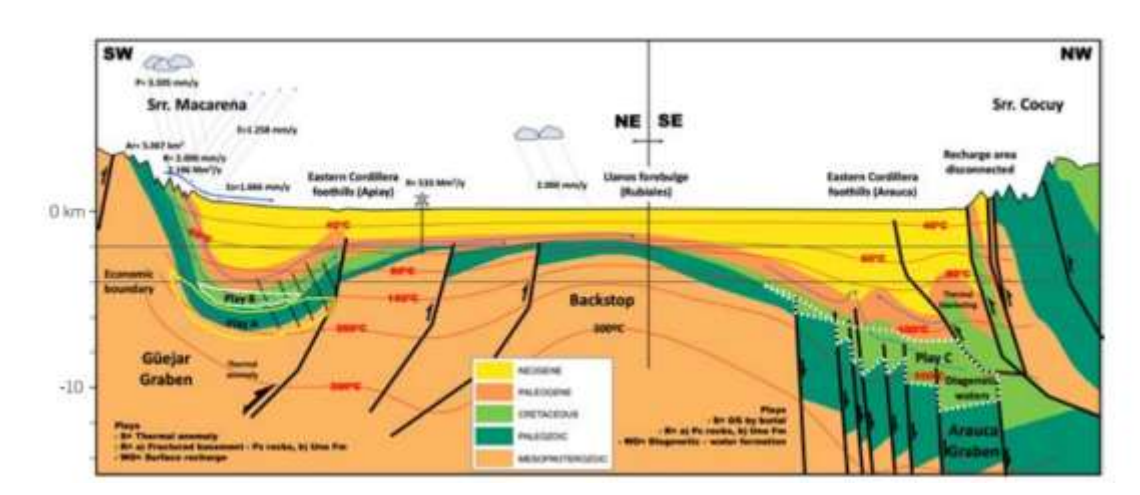


Figure 34. Conceptual hydrogeological model of the Llanos Basin showing recharge zones, fluid circulation, and geothermal plays defined in Figure 31 (from López-Ramos et al., 2022).

9 Economic Aspects and National Expectations

Colombia's energy vulnerability, together with governmental policies promoting sustainable development, has generated favorable conditions for the advancement of geothermal projects. Nevertheless, significant technical, legal, and financial barriers remain, particularly in early exploration stages (Moreno-Rendón et al., 2020). The country's electricity matrix is still dominated by hydropower and fossil fuels (EIA, 2018), while geothermal energy remains incipient, advancing mainly through pilot projects and exploratory studies.

Conduction-dominated geothermal resources based on oilfield co-produced waters represent an immediate opportunity for Colombia's energy transition. With an estimated technical potential of \sim 170 MWe, binary ORC plants of 200–320 kWe could achieve payback periods of 7–9 years under the current regulatory framework. Beyond their modest scale, these projects reduce operating costs in mature oil fields while supplying renewable electricity, turning a liability — produced water — into a strategic energy asset (Pinto et al., 2021) (Table 6).

Low and medium-enthalpy pilots have been developed in the Llanos Basin, where co-production of geothermal energy from oil fields offers a practical entry point. Parex Resources operates a project in Campo La Rumba (Casanare), generating 35 kW and supplying electricity to ~117 households (El Nuevo Oriente, 2024). Ecopetrol is developing a larger pilot in Chichimene (Meta), designed for 2 MW of installed capacity, enough to supply more than 6,000 homes (Jorquera, 2021). In addition, small-scale initiatives are under way in thermal spring areas and oil fields, while the first high-enthalpy concession was granted in 2025 for the Azufral volcano (Ecopetrol, 2025; SGC, 2025). These projects illustrate a dual pathway: co-production in sedimentary basins and stand-alone high-enthalpy developments in volcanic zones.

The Colombian Geological Survey (SGC) has mapped 21 geothermal areas associated with active and inactive volcanic systems, grouped into five prospective blocks: Paipa–Iza, San Diego–Cerro Bravo–Cerro Machín, Huila–Sucubún–Las Ánimas–Chiles, and the Azufral–Cumbal–Chiles–Cerro Negro sectors. Their assessment estimated a national geothermal potential of ~1170 MWe, corresponding only to convection-dominated systems with surface manifestations, based on a volumetric model and Montecarlo simulations (Alfaro et al., 2020). Historical global estimates ranged from 700–1370 MWe (Gawell et al., 1999) to 2210 MWe with improved drilling and stimulation techniques (Table 6, Figure 35).

Expectations for geothermal development are framed in the National Energy Plan (UPME, 2015, 2020), which projects the addition of 1398 MW from non-conventional renewables by 2028, of which 275 MWe

could come from geothermal plants. An optimistic scenario foresees 375 MWe installed by 2030, if the plan's strategic pillars—access, diversification, low emissions, and innovation—are achieved. In the longer term, projections suggest that by 2050 Colombia could install up to ~800 MW of geothermal capacity, consolidating the role of this resource in the national energy mix (Carreño et al., 2023).

Despite these expectations, several challenges persist. The cost of capital for geothermal energy in Colombia is ~2251 COP/kW, higher than solar or biomass but below hydropower (UPME, 2020). Technological uncertainty also remains high, given the country's limited experience in geothermal drilling and reservoir management. Moreover, resource quantification still requires detailed exploration to define reservoir size, physical properties, and fluid chemistry (ISAGEN, 2012).

Emerging approaches such as machine learning offer an opportunity to reduce exploration risk by modeling geothermal gradients and predicting reservoir properties from sparse datasets (Mejía-Fragoso et al., 2024). These advances, together with targeted pilot projects and regulatory incentives, could accelerate the transition from exploratory initiatives to a robust, sustainable geothermal industry in Colombia.

Table 6. Stored heat and estimated electrical potential of Colombian convection-dominated geothermal systems studied by Alfaro et al., 2020 and the conduction-dominated geothermal system studied by Pinto et al. (2021). Values were grouped into Paipa-Iza system, main volcanic complexes, secondary volcanic fields, other geothermal areas and conduction-dominated areas.

Group / Region	Heat (EJ)	Recoverable (EJ)	Potential (MWe)
Paipa–Iza system	~7.2	~0.8	~34
Major volcanic systems (Nevado del Ruiz, Tolima, Machín, Huila)	~42	~3.2	~440
Other volcanic complexes (Galeras, Azufral, Chiles, Cumbal, Sotará, etc.)	~34	~2.3	~240
Remaining convection-dominated geothermal areas	~55	~8.8	~456
Total (Convection-Dominated)	138.6	15.1	1170
Conduction-Dominated geothermal areas	_	_	170-287

Figure 35. Infographic on Colombia's geothermal potential and main pilot projects. Retrieved from https://www.piensageotermia.com/inaugurada-primera-planta-de-energia-geotermica-en-colombia/.

EL POTENCIAL ENERGÉTICO DE LA GEOTERMIA EN COLOMBIA 1.170 MW 138,60 Exa Joules Los sistemas geotérmicos se 000 Energía potencial encuentran asociados a estructuras 000 Recursos geotérmicos volcánicas o áreas de reciente del aprovechamiento aproximados en el país 000 del calor de la tierra actividad tectónica Departamentos con Proyectos pilotos Departamento SInversión Capacidad de generación mayor potencial de Campos Maracas Campo La Rumba Campo Chichimene generación con Desarrollado por Parex Desarrollado por Ecopetrol geotermia Casanare Aguazul, Casanare Acacías, Meta Caldas Tolima \$4.700 millones 5 0,035 MW 5 2 MW Risaralda Meta 72.000 kWh 672 kWh/día Antecedentes de la geotermia en Colombia Excavación requerida Empresas interesadas Volcanes con periferia Aprobación de la primera para evaluaciones y en geotermia de alta entalpía 1.994 licencia ambiental modelaciones Cerro Bravo Pucaré EPM Isagen Primera perforación De 1,5 a 3 km Enel San Diego Gemsa Galeras 1.997 del Nevado del Ruíz Ecopetrol Escondido de Florencia

10 Regulatory Framework

Colombia lacked a specific regulatory framework for geothermal energy until very recently, which created uncertainty for investors and limited the pace of project development (Martínez, 2021). Before 2022, geothermal resources were included under the broader category of non-conventional renewable energies (FNCER) and regulated mainly by Law 1715 of 2014, which promoted their integration into the national energy system. This law also established tax incentives—such as 50% deduction of investments, VAT exemptions on equipment, and accelerated depreciation of assets—later regulated through Decree 2143 of 2015, Decree 1543 of 2017 (FENOGE), Resolution 1283 of 2016, and Resolution 2000 of 2017.

The legal background extends further back: the Natural Resources Code (Decree-Law 2811 of 1974) and its 1978 reform defined geothermal resources as underground water naturally or artificially interacting with an endogenous heat source at temperatures above 80 °C, recognizing their potential uses for heating, electricity generation, and mineral recovery. Law 99 of 1993 created the National Environmental System (SINA) and environmental licensing procedures, while Law 697 of 2001 emphasized rational and efficient energy use.

The regulatory landscape advanced significantly with Law 2099 of 2021, which updated the provisions for the energy transition and explicitly included geothermal energy for both electricity generation and direct uses. This law reinforced the government's responsibility for geothermal resource assessment and project promotion.

A major milestone came with Decree 1318 of 2022, the first regulation dedicated exclusively to geothermal energy, which defined the technical and environmental guidelines for exploration and exploitation. More recently, Decree 1598 of 2024 established specific rules for project registration, environmental requirements, and concession procedures for both surface and groundwater use, explicitly recognizing geothermal as an independent energy source within the national portfolio.

Together, these norms position geothermal energy as a strategic alternative for Colombia's energy transition, supported by a progressively more robust institutional and legal framework (Alfaro and Rodríguez, 2020). However, the effective application of these instruments still depends on overcoming challenges in licensing, financing, and technical expertise, particularly in early exploration stages.

11 Social and Environmental Implications

The energy transition in Colombia, including the implementation of geothermal energy, involves a wide spectrum of social and environmental considerations. Corporate social responsibility (CSR) and compliance with constitutional principles on human and fundamental rights underpin the expectation that geothermal projects balance economic opportunities with social and environmental safeguards (García, 2021). Mining, construction, and transport sectors will play a key role by supplying materials, technologies, and labor, but their participation also implies new impacts on ecosystems and communities. The growing demand for strategic minerals (e.g., lithium, arsenic, silicon, iron) introduces both opportunities and risks, highlighting the need for responsible exploitation and circular economy practices.

Social acceptance of geothermal energy in Colombia is broadly favorable. Balzan-Alzate et al. (2021) report that ~85% of respondents support electricity generation from geothermal resources, though acceptance decreases when hydraulic stimulation is proposed. The main conditions expressed by communities are linked to environmental protection, safety, and meaningful participation in decision-making. Despite relatively low public awareness compared to other countries, this evidence suggests a socially favorable setting for geothermal development, provided that adequate communication, transparency, and participatory mechanisms are in place.

From the environmental perspective, the scale and nature of impacts depend on the type of system. High-enthalpy plants may cause emissions of CO₂ and H₂S, noise during drilling and operation, and localized visual impacts, but these are minimal compared to fossil fuels and can be mitigated through proper technology. Direct uses of geothermal fluids raise risks of chemical pollution (e.g., boron, arsenic, mercury) and thermal pollution if fluids are discharged untreated into surface ecosystems. Modern practices—reinjection wells, dilution, cooling, and reverse osmosis—offer proven mitigation. Hydrothermal alteration and mineral mobilization also necessitate early monitoring to prevent contamination of groundwater and soils (Martínez, 2021).

Environmental licensing ensures oversight of these risks. Under Colombian law, geothermal projects are subject to licenses granted by the National Environmental Licensing Authority (ANLA) for capacities above 100 MWe, while projects between 10 and 100 MWe are evaluated by the Regional Autonomous Corporations (CARs). Licenses require developers to comply with prevention, mitigation, compensation, and monitoring measures, and explicitly prohibit development in protected areas of the National System of Protected Areas (SINAP) (Law 99 of 1993; Law 2099 of 2021).

Colombia's post-conflict context adds a further layer: geothermal exploration often occurs in territories historically affected by armed conflict, where accessibility, community trust, and governance remain fragile. Integrating geothermal projects into local development agendas with clear commitments to security, employment, and benefit sharing is therefore essential. Finally, the challenge of misinformation underscores the need for consistent, transparent communication and community engagement, enabling constructive participation in project design and decision-making (Martínez-Ruiz et al., 2021).

In summary, while geothermal energy offers Colombia a low-carbon, locally available, and relatively clean alternative, its successful deployment depends on aligning environmental management with strong social engagement. The combination of favorable public perception, regulatory oversight, and emerging pilot projects suggests that Colombia has the social license and institutional tools necessary to advance geothermal development as part of its energy transition.

Discussion

Colombia's geothermal potential is strongly linked to its geodynamic context within the Andean volcanic belt and the structural complexity of its sedimentary basins. Volcanic systems such as Nevado del Ruiz, Azufral, and the Tufiño-Chiles-Cerro Negro complex, together with the non-volcanic Paipa system, have been consistently highlighted as priority targets (Mejía et al., 2014; Salazar et al., 2017; Alfaro et al., 2020). Recent developments reinforce this outlook: the first geothermal generation was achieved in Campo Maracas (2024), and in 2025 the government granted exploration permits at Azufral, marking a potential milestone for high-enthalpy exploitation (SGC, 2025; Ecopetrol, 2025).

While Alfaro et al. (2020) estimated ~1170 MWe from convective systems with surface manifestations, and Pinto et al. (2021) added preliminary figures for conduction-dominated settings, these remain indicative rather than definitive, given the absence of deep exploration wells. Comparisons with other countries underscore both opportunities and challenges: while the United States exceeds 3700 MWe of installed capacity and Mexico surpasses 1000 MWe (Lund & Toth, 2021), Colombia has yet to advance beyond pilot projects. This contrast illustrates the gap between geological promise and technological—institutional maturity.

Several uncertainties constrain geothermal development in Colombia. Variability in reported geothermal gradients and reservoir temperatures across studies reflects both geological heterogeneity and the scarcity of direct subsurface data (Alfaro et al., 2009; Quintero et al., 2019; Matiz-León, 2023; Mejía-Fragoso et al., 2024). Most temperature and gradient estimates are based on geothermometers, indirect geophysics, or predictive models, which emphasizes the need for exploratory drilling to validate conceptual models and reduce risk.

Beyond these conventional prospects, blind geothermal systems represent an additional opportunity. International experience shows that reservoirs without surface manifestations can still be highly productive. The Brawley field in California was delineated through distributed acoustic sensing in fiber optics (Cheng et al., 2023), while in the Great Basin, Nevada, blind systems have been identified using gravity anomalies and 3D geological modeling (Ward & Sellars, 2024). Similar data-driven approaches have revealed fossil and hidden geothermal systems in Nigeria's Yankari Park via satellite mineral mapping (Abubakar et al., 2019), geothermal manifestation patterns at Desert Peak, Nevada, using Aldriven remote sensing (Moraga et al., 2022) and previously unmeasured geothermal gradients in Colombia (Mejía-Fragoso et al., 2024). These examples suggest that Colombia's resource base may be underestimated if exploration focuses solely on visible manifestations or conservative approaches, highlighting the need for advanced geophysical, geochemical, remote sensing and data-driven techniques to expand the geothermal portfolio.

Policy and regulatory advances—such as Law 2099 (2021) and subsequent decrees—have begun to reduce legal uncertainty, but additional measures are required to attract private investment and mitigate high exploration costs. Strategic incentives, improved financing mechanisms, and the integration of geothermal into the National Energy Plan (UPME, 2020) are essential. Furthermore, the application of innovative approaches, including machine learning for geothermal gradient prediction (Mejía-Fragoso et al., 2024), could improve early-stage assessments and optimize resource targeting.

In this context, geothermal energy in Colombia should be seen not only as a clean baseload option but also as a driver for regional development through direct uses such as balneology, agriculture, and industrial applications. The transition from pilot projects to commercial plants will depend on bridging the exploration gap, consolidating institutional support, and demonstrating technical feasibility in diverse geological settings. Beyond the technical and regulatory dimensions, geothermal development in Colombia faces economic and social challenges. High upfront costs and limited financial instruments constrain competitiveness compared to other renewables, though oilfield co-production projects offer a transitional pathway to reduce investment risks. Public perception is broadly favorable, with more than 80% of respondents supporting geothermal electricity generation when environmental safeguards and community benefits are guaranteed (Balzan-Alzate et al., 2021). Looking ahead, optimistic scenarios under the National Energy Plan project up to 800 MWe installed by 2050 (Carreño et al., 2023). These perspectives highlight geothermal energy not only as a low-carbon baseload alternative, but also as a catalyst for regional development through direct uses, innovation, and integration into Colombia's broader energy transition.

Conclusion

Colombia's geodynamic setting within the Andean belt, combined with the structural complexity of its sedimentary basins, offers favorable conditions for geothermal development. Volcanic systems such as Nevado del Ruiz, Azufral, and Tufiño–Chiles–Cerro Negro, together with non-volcanic prospects like Paipa, illustrate the diversity of geothermal environments present in the country.

The reviewed literature confirms reservoir temperatures frequently exceeding 200 °C, highlighting the potential for high-enthalpy exploitation in volcanic complexes and for medium- to low-enthalpy uses in sedimentary and oilfield contexts. Nonetheless, the sector remains underexplored: most assessments rely on indirect geophysical and geochemical methods, while deep drilling and reservoir testing are still scarce. This knowledge gap sustains high levels of geological and financial uncertainty.

Future progress will depend on three factors: (i) reducing exploration risk through detailed structural characterization, reservoir drilling, and innovative tools such as machine-learning-based gradient modeling; (ii) consolidating a stable regulatory and financial framework that incentivizes private investment; and (iii) integrating geothermal into broader energy and territorial development strategies,

including direct uses such as balneology, heating, and agro-industrial applications.

In summary, geothermal energy in Colombia represents both a challenge and an opportunity. While geological evidence and initial pilots demonstrate promising conditions, realizing this potential will require sustained research, institutional support, and community engagement. If these conditions are met, geothermal energy can evolve from isolated initiatives to a reliable component of Colombia's clean energy transition and a reference point for the region.

References

- [1] Abubakar, A., Hashim, M., & Pour, A. (2019). Identification of hydrothermal alteration minerals associated with geothermal system using ASTER and Hyperion satellite data: a case study from Yankari Park, NE Nigeria. Geocarto International, 34, 597 625. https://doi.org/10.1080/10106049.2017.1421716.
- [2] Aguilera, P., Alfaro, C., Arcila, A., Blessent, D., Rueda, J., Llamosa, O. (2019, November). Colombia-a geothermal opportunity. In *41st New Zealand Geothermal Workshop* (Vol. 11).
- [3] Alfaro, C. (2002). Geoquímica del sistema geotérmico de Paipa. Ingeominas, informe inédito. Bogotá, 88.
- [4] Alfaro, C. M., Rueda Gutiérrez, J. B., Casallas, Y. P., Rodríguez, G. Z., and Malo, J. E. (2020). Estimación preliminar del potencial geotérmico de colombia. Technical report, Servicio Geológico Colombiano, Bogotá.
- [5] Alfaro, C., Alvarado, I., Quintero, W., Hamza, W., Vargas, C., Briceño, L. (2009). Preliminary map of geothermal gradients in Colombia. In *XII Colombian Congress of Geology* (pp. 1-24).
- [6] Alfaro, C., Garzón, G., Bobadilla, L. (2008). Geoquímica preliminar de gases del sistema geotérmico del volcán Azufral. Geología colombiana, 33, 91-98.
- [7] Alfaro, C., Garzón, G., Bobadilla, L. (2008). Geoquímica preliminar de gases del sistema geotérmico del volcán Azufral. Geología colombiana, 33, 91-98.
- [8] Alfaro, C., Ponce, P., Monsalve, M. L., Ortiz, I., Franco, J. V., Ortega, A., ... & Gómez, D. (2015, April). A preliminary conceptual model of Azufral geothermal system, Colombia. In *Proceedings World Geothermal Congress* (pp. 10p-10p).
- [9] Alfaro, C., Rodríguez-Rodríguez, G. (2020). Status of the geothermal resources of Colombia: Country Update. In Proceedings, World Geothermal Congress.
- [10] Alfaro, C., Velandia, F., Cepeda, H., Pardo, N. (2010). Preliminary conceptual model of the Paipa geothermal system, Colombia. In Proceedings World Geothermal Congress.
- [11]Alfaro-Valero, C. M., Rueda-Gutiérrez, J. B., Matiz-León, J. C., Beltrán-Luque, M. A., Rodríguez-Rodríguez, G. F., Rodríguez-Ospina, G. Z., Malo-Lázaro, J. E. (2020). Paipa geothermal system, Boyacá: Review of exploration studies and conceptual model. The Geology of Colombia, 4, 161-196.
- [12]ANH (Agencia Nacional de Hidrocarburos), 2010a. Llanos orientales. https://www.anh.gov.co/es/hidrocarburos/oportunidades-disponibles/procesosdeseleccion/ronda-colombia-2010/tipo-1/llanos-orientales/.
- [13]ANH (Agencia Nacional de Hidrocarburos), 2010b. Valle medio del magdalena. https://www.anh.gov.co/es/hidrocarburos/oportunidades-

- disponibles/procesosdeseleccion/ronda-colombia-2010/tipo-1/valle-medio-del-magdalena/.
- [14] Bachu, S., Ramon, J. C., Villegas, M. E., & Underschultz, J. R. (1995). Geothermal regime and thermal history of the Llanos Basin, Colombia. AAPG bulletin, 79(1), 116-128.
- [15]Balzan-Alzate, D., López-Sánchez, J., Blessent, D., Raymond, J., Dezayes, C., Portela, J. P., ... & Le Borgne, T. (2021). An online survey to explore the awareness and acceptance of geothermal energy among an educated segment of the population in five European and American countries. *Geothermal Energy*, 9(1), 9.
- [16]Barrero, D., Pardo, A., Vargas, C.A., Martínez, J.F., 2007. Colombian Sedimentary Basins: Nomenclature, Boundaries and Petroleum Geology, a New Proposal, Vol. 1. Agencia Nacional de Hidrocarburos, p. 9
- [17]Bayona, G., Cardona, A., Jaramillo, C., Mora, A., Montes, C., Valencia, V., Ayala, C., Montenegro, O., and Ibañez-Mejia, M. 2012. Early Paleogene magmatism in the northern Andes: Insights on the effects of Oceanic Plateau—continent convergence. Earth and Planetary Science Letters, 331-332: 97-111.
- [18] Bertrami, R., Camacho, A. De Stefanis, L., Medina, T., Zuppi, G.M. 1992. Geochemical and isotopic exploration of the geothermal area of Paipa, Cordillera Oriental, Colombia. Estudios geotérmicos con técnicas isotópicas y geoquímicas en América Latina. OIEA. Viena. 457 pp.
- [19]Bocanegra, L. C., Sánchez, J. J. (2017). Mapa de fallas de los volcanes Chiles-Cerro Negro (Nariño) a partir de minería de datos y confirmación de campo. Boletín de Geología, 39(3), 71-86.
- [20]Bona, P., Coviello, M. F. (2016). Valoración y gobernanza de los proyectos geotérmicos en América del Sur. Una propuesta metodológica. Comisión Económica para América Latina y el Caribe (CEPAL)
- [21] Borrero, C., Toro, L. M., Alvarán, M., Castillo, H. (2009). Geochemistry and tectonic controls of the effusive activity related with the ancestral Nevado del Ruiz volcano, Colombia. *International Geophysics*, 48(1), 149-169.
- [22] Carreño, D., Dyner, I., Sanint, E., & Aristizábal, A. (2023). Prospectiva de la geotermia en Colombia hacia 2050. [Informe de investigación]. Universidad Nacional de Colombia.
- [23] Carvajal, D., Alfaro, C., Mendoza, J. C. M., Romero, D., Mojica, J. (2008). Contribución al Modelo Geotérmico del Volcán Azufral a partir de identificación de zonas de Alteración Hidrotermal. Geología Colombiana, 33, 99-108.
- [24] Ceballos-Hernández, J.A., Martínez-Tabares, L.M., Valencia-Ramírez, L.G., Pulgarín-Alzate, B.A., Correa-Tamayo, A.M. & Narváez-Marulanda, B.L. 2020. Geological evolution of the Nevado del Ruiz Volcanic Complex. In: Gómez, J. & Pinilla-Pachon, A.O. (editors), The Geology of Colombia, Volume 4 Quaternary. Servicio Geológico Colombiano, Publicaciones Geológicas Especiales 38, p. 267–296. Bogotá. https://doi.org/10.32685/pub.esp.38.2019.07
- [25] Cheng, F., Ajo-Franklin, J., Nayak, A., Tribaldos, V., Mellors, R., & Dobson, P. (2023). Using Dark Fiber and Distributed Acoustic Sensing to Characterize a Geothermal System in the Imperial Valley, Southern California. Journal of Geophysical Research: Solid Earth, 128. https://doi.org/10.1029/2022JB025240.
- [26] Cortés, G. P. y Calvache, M. L. (1996). Geología de los volcanes Chiles y Cerro Negro. Informe interno. San Juan de Pasto: Ingeominas.

- [27] Cortés, G. P., Monsalve, M. L., Narváez, P. A. y Muñoz, C. J. (2023). Mapa de amenaza volcánica del Complejo Volcánico Chiles Cerro Negro Memoria explicativa. Pasto: Servicio Geológico Colombiano.
- [28] Coviello, M. (2000). Estudio para la evaluación del entorno del Proyecto Geotérmico Binacional" Tufiño-Chiles-Cerro Negro".
- [29]de Porta, J. (2003). La formación del istmo de Panamá. Su incidencia en Colombia.
- [30] Ecopetrol. (2025, julio 11). Ecopetrol inicia proyecto de exploración geotérmica en Nariño, una fuente estratégica de energía. Ecopetrol. https://www.ecopetrol.com.co/wps/portal/Home/es/noticias/detalle/ecopetrol-inicia-procesopara-comercializar-entre-12-y-26-gbtud-de-gas-del-campo-florena
- [31]EIA (Energy Information Administration), 2018. https://www.eia.gov/international/analysis/country/COL. Ultimo acceso 30 mayo 2025.
- [32] Federico; C., Inguaggiato, S., Chacón, Z., Makario Londoño, J-., Gil, E., Alzate, D. (2017). Vapour discharges on Nevado del Ruiz during the recent activity: Clues on the composition of the deep hydrothermal system and its effects on thermal springs. *Journal of Volcanology and Geothermal Research*, 346: 40-53.
- [33] Forero Herrera, J. A. (2012). Caracterización de las alteraciones hidrotermales en el flanco Noroccidental del Volcán Nevado del Ruiz, Colombia. *Departamento de Geociencias*.
- [34]García Lara, A. V. (2021). Caracterización mineralógica de las alteraciones hidrotermales en el área geotérmica de Paipa Boyacá, Colombia.
- [35]García Moreno, A. C. (2021). Responsabilidad social empresarial en el sector minero de cara a la transición energética en Colombia.
- [36] García, R. D., Gutiérrez, S. L., Pareja, E. R., Pusquin, L. T., Dewhurst, W. T., López, J. P. (2013). Case Study and First Look: Contemporary Magnetotelluric Studies Within Nereidas Valley, Nevado del Ruiz Volcano, Colombia. *Geothermal Resources Council Transactions*, 37.
- [37]García, Y. K., Sánchez, J. J. (2019). Contribuciones geológicas al modelo conceptual geotérmico en la región de los volcanes Chiles-Cerro Negro (Colombia-Ecuador). Boletín de Geología, 41(1), 151-171.
- [38] Gawell, K., Reed, M., Wright M. (1999). Preliminary Report: Geothermal Energy, the Potential for Clean Power from the Earth. Geothermal Energy Association Report.
- [39] Giggenbach, W.F, Goguel R.L. (1991). Collection and analysis of geothermal and volcanic water and gas discharges. Internal Report No. CD 2401, Chemistry Div., Dep. Sci. and Ind. Res., Petone, New Zealand, 81 p.
- [40]Gómez Romero, D. A. (2019). Modelo geotérmico de Paipa mediante exploración del subsuelo y análisis físico químico de aguas termales (Doctoral dissertation, Universidad Pedagógica y Tecnológica de Colombia).
- [41]Gómez, J., Montes, N.E., Nivia, A., Diederix, H., 2015. Mapa geológico de Colombia. Escala, 1:1.000.000. https://datos.sgc.gov.co/maps/ c05c6dbf27f645eb883bae3a9cd0d08f.
- [42]Gómez-Tapias J., Núñez-Tello A., Mateus-Zabala D., Alcárcel-Gutiérrez F.A., Lasso-Muñoz R.M., Marín-Rincøn E., Marroquín M., Zabala M. Physiographic and geological setting of the

- Colombian territory. Geol. Colombia, 1 (2020), pp. 1-6, 10.32685/pub.esp.35.2019.01
- [43]González, H.; Zapata G.; Montoya, D. (2002). Geología y Geomorfología de la plancha 428 Túquerres. INGEOMINAS, Medellín.
- [44]González-Garcia, J., Hauser, J., Annetts, D., Franco, J., Vallejo, E., & Regenauer-Lieb, K. (2015). Nevado Del Ruiz Volcano (Colombia): a 3D model combining geological and geophysical information. In *Proceedings of the World Geothermal Congress* (pp. 1-11).
- [45]González-Idárraga, C. E. (2020). Caracterización resistiva 3D del área geotérmica de Paipa, Colombia. *Boletín de Geología*, *42*(3), 81-97.
- [46]IEA (2024), The Future of Geothermal Energy, IEA, Paris https://www.iea.org/reports/the-future-of-geothermal-energy, Licence: CC BY 4.0
- [47] INGEOMINAS (1997). Nereidas Well Geology Report. Geoenergía Andina S.A. Contract. GESA. Product. Version year 1997. Report 2288.
- [48]INGEOMINAS and ANH, 2009. MAPA PRELIMINAR DE GRADIENTES GEOTÉRMICOS DE COLOMBIA.. Report. Bogotá. 34p.
- [49]Instituto Colombiano de Energía Eléctrica ICEL (1983). Proyecto Geotérmico Chiles-Cerro Negro. Fase I Etapa de prefactibilidad. Informe preliminar. 159p.
- [50]ISAGEN, S. (2012). Notas para la investigación y desarrollo de proyectos geotérmicos en Colombia. 78p.
- [51] Jorquera, C. (2021). Inaugurada primera planta de energía geotérmica en Colombia. Recuperado de https://www.piensageotermia.com/inaugurada-primera-planta-de energia-geotermica-en-colombia/
- [52]Linares Correal, Y. A. (2013). Apoyo al estudio geotérmico del Volcán Nevado del Ruiz mediante el análisis de fluidos no condensados provenientes de manantiales termales y de fumarolas volcánicas (Doctoral dissertation).
- [53] Lobo-Guerrero, A. (1987). La geología de Colombia. INGEOMINAS, 8p.
- [54] López, D. A. L. (1992). The hydrothermal system of Nevado del Ruiz Volcano, Colombia (Doctoral dissertation, Louisiana State University and Agricultural & Mechanical College).
- [55]López-Ramos, E., Gonzalez-Penagos, F., Patiño, C. A., & López, A. (2022). Low-medium enthalpy geothermal resource assessment in deep reservoirs of the Llanos Basin-Colombia. CT&F-Ciencia, Tecnología y Futuro, 12(1), 13-44.
- [56] Lund, J. W., Toth, A. N. (2021). Direct utilization of geothermal energy 2020 worldwide review. Geothermics, 90, 101915.
- [57] Martínez Martínez, J. A. (2021). Marco jurídico sobre la generación de energía geotérmica en Colombia.
- [58] Martínez, L.M., Valencia, L.G., Ceballos, J.A., Narváez, B.L., Pulgarín, B.A., Correa, A.M., Navarro, S., Murcia, H.F., Zuluaga, I., Rueda, J.B. & Pardo, N. 2014. Geología y estratigrafía del Complejo Volcánico Nevado del Ruiz. Servicio Geológico Colombiano, unpublished report, 403 p. Bogotá.
- [59]Martínez-Ruiz, Y., Manotas-Duque, D. F., Ramírez-Malule, H. (2021). Análisis de opciones

- reales para la valoración financiera de proyectos de energía geotérmica en Colombia. Revista CEA, 7(15), e1944-e1944.
- [60]Matiz-León, J. C. (2023). Spatial Prediction for Bottom Hole Temperature and Geothermal Gradient in Colombia. In Proceedings of the 48th Workshop on Geothermal Reservoir Engineering, Stanford University, Stanford, California, February 6-8, 2023 (SGP-TR-224).
- [61] Mejía, E. L., Velandia, F., Zuluaga, C. A., López, J. A., Cramer, T. (2012). Structural analysis northeast of the Nevado del Ruíz volcano, Colombia-Contribution to geothermal exploration. Geology Bulletin, 34(1), 27-41.
- [62] Mejía, E., Rayo, L., Méndez, J., Echeverri, J. (2014). Geothermal development in Colombia. Short Course VI on Utilization of Low-and Medium-Enthalpy Geothermal Resources and Financial Aspects of Utilization, Santa Tecla, El Salvador, 1-7.
- [63] Mejía-Fragoso, J. C., Florez, M. A., & Bernal-Olaya, R. (2024). Predicting the geothermal gradient in Colombia: A machine learning approach. *Geothermics*, *122*, 103074.
- [64] Moraga, J., Duzgun, H., Çavur, M., & Soydan, H. (2022). The Geothermal Artificial Intelligence for geothermal exploration. Renewable Energy. https://doi.org/10.1016/j.renene.2022.04.113.
- [65] Moreno Rendón, D. A. M., Sánchez, I. J. L., Blessent, D. (2020). Geothermal energy in Colombia as of 2018. Ingeniería y Universidad, 24, 6.
- [66] Moreno Rendón, D., Lopez-Sanchez, J., Blessent, D., Raymond, J. (2018). Fault characterization and heat-transfer modeling to the Northwest of Nevado del Ruiz Volcano. Journal of South American Earth Sciences, 88, 50-63.
- [67]OLADE (1987). Proyecto Geotérmico Binacional Tufiño-Chiles-Cerro Negro, Informe Final, Aquater spa.
- [68]Ovalle, J. A. (2020). Geotermia en la región central. Convenio Interadministrativo 080 de 2019. Región Administrativa y de Planeación Especial RAP-E - Universidad Distrital Francisco José de Caldas.
- [69] Partida, E. G., Gómez, V. M. A., Reyes, R. M. B., Birkle, P., & Rodríguez, V. T. (1997). Comportamiento geoquímico de las manifestaciones geotérmicas en el flanco oriental del volcán El Nevado del Ruiz (Río Claro-Las Nereidas), Colombia. *Tecnología y ciencias del* agua, 12(3), 5-13.
- [70]Pinto, O., & Congress, W. G. (2021). Towards the Use of Geothermal Resources Available in Oil and Gas Sedimentary Basins in Colombia. In *Proceedings World Geothermal Congress. Reykjavik* (p. 11).
- [71]Ponce, P., 2013. Exploración de Recursos Geotérmicos del Volcán Azufral a partir de la interpretación de Anomalías de Campos Potenciales. Universidad Nacional de Colombia. Tesis de Maestría. Pasto.
- [72]Presidencia de la República de Colombia. (2022, julio 27). DECRETO 1318 DE 2022: Por el cual se adiciona el Decreto 1073 de 2015 Único Reglamentario del Sector Administrativo de Minas y Energía, con el fin de reglamentar los artículos 21 y 21-1 de la Ley 1715 de 2014 en lo relacionado con el desarrollo de actividades orientadas a la generación de energía eléctrica a través de geotermia.
- [73] Presidencia de la República de Colombia. (2024, diciembre 27). Decreto 1598 de 2024: Por

- el cual se modifica el Decreto 1073 de 2015, en relación con el desarrollo de actividades orientadas a la generación de energía eléctrica a través de geotermia y se establecen otras disposiciones.
- [74] Quintero, W., Campos-Enríquez, O., & Hernández, O. (2019). Curie point depth, thermal gradient, and heat flow in the Colombian Caribbean (northwestern South America). Geothermal Energy, 7(1), 1-20.
- [75]Rangel Jurado, N. (2017) Contribución al estudio del potencial geotérmico del Volcán Azufral mediante la caracterización geoquímica de fluidos provenientes de manantiales termales y la aplicación de geotermometría en fase líquida. Trabajo de grado. Universidad de los Andes, Bogotá.
- [76] Rayo-Rocha, L., Zuluaga, C. A. (2011). Magmatic processes at Nevado del Ruiz volcano: A textural quantitative analysis. Geology Bulletin, 33(2), 59-72.
- [77]Rodríguez Rodríguez, G. F., & Vallejo Rodríguez, E. F. (2013). Sondeos Térmicos Superficiales en el Área Geotérmica de Paipa (Boyacá). Colombian Geological Survey. Research and Exploration of Geothermal Resources, Basic Geology, Bogotá, Colombia.
- [78] Rodríguez-Rodríguez, G. (2023). Aportes a la investigación del sistema geotérmico del volcán Azufral en Colombia mediante modelos 2D de magnetotelúrica. *Boletín de Geología*, *45*(2), 51-63.
- [79] Salazar, S. S., Muñoz, Y., Ospino, A. (2017). Analysis of geothermal energy as an alternative source for electricity in Colombia. Geothermal Energy, 5(1), 1-12.
- [80] Sarmiento, O. E. (2014). Aplicación de una metodología de procesamiento e interpretación de información magnetotelúrica sobre varios perfiles localizados en la zona occidental del volcán nevado del ruíz-colombia. *Boletín de Geología*, 36(1), 57-70.
- [81] Schaefer, S. J. (1995). Nevado del Ruiz volcano, Colombia: magmatic system and evolution. Arizona State University.
- [82]Servicio Geológico Colombiano. (2025, julio 11). Lo que debe saber sobre la energía geotérmica en Colombia y el volcán Azufral. SGC. https://www2.sgc.gov.co/Noticias/Paginas/Lo-que-debe-saber-sobre-la-energia-geotermica-en-Colombia-y-el-volcan-Azufral.aspx
- [83]Servicio Geológico Colombiano. (2025, mayo 14). ¿Qué está pasando con la geotermia en Colombia? SGC. https://www2.sgc.gov.co/Noticias/Paginas/Que-esta-pasando-con-la-geotermia-en-Colombia.aspx
- [84]SGC (2016). Actualización del modelo geotérmico conceptual del área geotérmica de Paipa. In Simposio Grupo Exploración de Recursos Geotérmicos [online].
- [85] Taussi, M., Tardani, D., Tassi, F., Gorini, A., Aguillera, E., Capaccioni, B., & Renzulli, A. (2023). A conceptual model for the Tufiño-Chiles-Cerro Negro (TCCN) geothermal system (Ecuador-Colombia): New insights into geothermal exploration from chemical and isotopic composition of hydrothermal fluids. *Journal of Geochemical Exploration*, 249, 107214.
- [86] Thouret, J.C., Cantagrel, J.M., Salinas, R. & Murcia, A. 1990. Quaternary eruptive history of Nevado del Ruiz, Colombia. Journal of Volcanology and Geothermal Research, 41(1–4): 225–251. https://doi.org/10.1016/0377-0273(90)90090-3

- [87] Torres, P., Cortés, G., Calvache, M., Monsalve, M. L. (2001). Geología y Estratigrafía del Volcán Azufral, Colombia. VIII Congreso Colombiano de Geología, Manizales.
- [88] Torres, P., Cortés, G., Calvache, M., Monsalve, M. L. (2001). Geología y Estratigrafía del Volcán Azufral, Colombia. VIII Congreso Colombiano de Geología, Manizales.
- [89] UPME (2015). PLAN ENERGETICO NACIONAL COLOMBIA: IDEARIO ENERGÉTICO 2050.
- [90] UPME (2020). Plan Energético Nacional 2020-2050.
- [91] Vargas, S., Dewhurst, W. (2014). Reconnaissance Analysis of a Geothermal System within the Central Cordillera of Colombia: Nevado del Ruiz. Geothermal Resources Council Transactions, 38.
- [92]Vélez, M. I., Blessent, D., Córdoba, S., López-Sánchez, J., Raymond, J., Parra-Palacio, E. (2017). Geothermal potential assessment of the Nevado del Ruiz volcano based on rock thermal conductivity measurements and numerical modeling of heat transfer. Journal of South American Earth Sciences, 81, 153-164.
- [93]Ward, O., & Sellars, J. (2024). Pioneering the Future of Geothermal Energy: a Case Study from the Great Basin Region. 85th EAGE Annual Conference & Exhibition (including the Workshop Programme). https://doi.org/10.3997/2214-4609.2024101343.